

SYNTHESIS OF A NOVEL SERIES OF FURAN AND FLUORENE
CONTAINING MONOMERS AND THEIR POLYMERS

A THESIS SUBMITTED TO
THE GRADUATE SCHOOL OF NATURAL AND APPLIED SCIENCES
OF
MIDDLE EAST TECHNICAL UNIVERSITY

BY

ARZU GÜNEŞ

IN PARTIAL FULFILLMENT OF THE REQUIREMENTS
FOR
THE DEGREE OF MASTER OF SCIENCE
IN
POLYMER SCIENCE AND TECHNOLOGY

SEPTEMBER 2011

Approval of the thesis:

**SYNTHESIS OF A NOVEL SERIES OF FURAN AND FLUORENE
CONTAINING MONOMERS AND THEIR POLYMERS**

submitted by **ARZU GÜNEŞ** in partial fulfillment of the requirements for the degree of **Master of Science in Polymer Science and Technology Department, Middle East Technical University** by,

Prof. Dr. Canan Özgen
Dean, Graduate School of **Natural and Applied Sciences** _____

Prof. Dr. Necati Özkan
Head of Department, **Polymer Science and Technology** _____

Prof. Dr. Ahmet M. Önal
Supervisor, **Polymer Science and Tech. Dept., METU** _____

Assoc. Prof. Dr. Atilla Cihaner
Co-Supervisor, **Chemical Engineering and Applied Chemistry Dept., Atılım Uni.** _____

Examining Committee Members:

Prof. Dr. Teoman Tinçer
Polymer Science and Technology Dept., METU _____

Prof. Dr. Ahmet M. Önal
Polymer Science and Technology Dept., METU _____

Assoc. Prof. Dr. Atilla Cihaner
Chemical Eng. and Applied Chemistry Dept., Atılım Uni. _____

Assist. Prof. Dr. H. Emrah Ünal
Metallurgical and Materials Engineering Dept., METU _____

Assist. Prof. Dr. Ali Çırpan
Polymer Science and Technology Dept., METU _____

Date: September 16, 2011

I hereby declare that all information in this document has been obtained and presented in accordance with academic rules and ethical conduct. I also declare that, as required by these rules and conduct, I have fully cited and referenced all materials and results that are not original to this work.

Name, Last name: Arzu Güneş

Signature:

ABSTRACT

SYNTHESIS OF A NOVEL SERIES OF FURAN AND FLUORENE CONTAINING MONOMERS AND THEIR POLYMERS

Güneş, Arzu

M.Sc., Department of Polymer Science and Technology

Supervisor: Prof. Dr. Ahmet M. Önal

Co-Supervisor: Assoc. Prof. Dr. Atilla Cihaner

September 2011, 65 pages

In this study, a novel series of conjugated monomers containing furan and fluorene units; 2,7-di(furan-2-yl)-9H-fluoren-9-one (FOF), 2-(2-(furan-2-yl)-9H-fluoren-7-yl)furan (FFF), and 2-(2-(furan-2-yl)-9,9-dihexyl-9H-fluoren-7-yl)furan (FHF) were synthesized and their electrochemical polymerization were achieved via potential cycling. Optical and electrochemical properties of the polymers, poly(2,7-di(furan-2-yl)-9H-fluoren-9-one) (PFOF), poly(2-(2-(furan-2-yl)-9H-fluoren-7-yl)furan (PFFF) and poly(2-(2-(furan-2-yl)-9,9-dihexyl-9H-fluoren-7-yl)furan (PFHF) were investigated and it was found that polymer films exhibit reversible redox behavior ($E_p^{ox} = 1.083$ V for PFOF, $E_p^{ox} = 0.915$ V for PFFF and $E_p^{ox} = 0.985$ V for PFHF) accompanied with a reversible electrochromic behavior, orange to green for PFOF, yellow to dark blue for PFFF and orange to green for PFHF during oxidation. Their band gap values (E_g) were found to be 2.32, 2.49 and 2.61 eV for PFOF, PFFF and PFHF, respectively.

Keywords: Conjugated polymer, Donor-acceptor system, Furan, Fluorene, Electrochromism.

ÖZ

FURAN VE FLOREN BİRİMLERİ İÇEREN YENİ MONOMERLERİN SENTEZİLERİ VE POLİMERLEŞTİRİLMELERİ

Güneş, Arzu

Yüksek Lisans, Polimer Bilimi ve Teknolojisi Bölümü

Tez Yöneticisi: Prof. Dr. Ahmet M. Önal

Ortak Tez Yöneticisi: Doç. Dr. Atilla Cihaner

Eylül 2011, 65 sayfa

Bu çalışmada, furan ve florene birimleri içeren yeni konjüge monomerler serisi; 2,7-di(furan-2-yl)-9H-floren-9-one (FOF), 2-(2-(furan-2-yl)-9H-floren-7-yl)furan (FFF), and 2-(2-(furan-2-yl)-9,9-dihexzil-9H-floren-7-yl)furan (FHF) sentezlenmiş ve döngülü voltametri ile elektrokimyasal olarak polimerleştirilmiştir. Elde edilen polimerlerin, poly(2,7-di(furan-2-yl)-9H-fluoren-9-one) (PFOF), poly(2-(2-(furan-2-yl)-9H-floren-7-yl)furan) (PFFF) ve poly(2-(2-(furan-2-yl)-9,9-dihexzil-9H-floren-7-yl)furan) (PFHF), optik ve elektrokimyasal özellikleri incelenmiş ve polimer filmlerinin tersinir redoks davranımı yanısıra (PFOF için $E_p^{ox} = 1.083$ V , PFFF için $E_p^{ox} = 0.915$ V ve PFHF için $E_p^{ox} = 0.985$ V); yükseltgenme sırasında PFOF için turuncudan yeşile, PFFF için sarıdan koyu maviye ve PFHF için turuncudan yeşile, ile sonuçlanan tersinir elektrokromik davranımı gösterdiği tespit edilmiştir. PFOF, PFFF ve PFHF için bant aralıkları sırasıyla 2.32, 2.49 ve 2.61 eV olarak bulunmuştur.

Anahtar Sözcükler: Konjüge Polimer, Elektron verici-alıcı sistem, Furan, Floren, Elektrokromizm.

To My Family ...

ACKNOWLEDGEMENTS

I would like to express my deepest gratitude to my supervisor Prof. Dr. Ahmet M. ÖNAL since he was always so polite in every step of the thesis and also he encouraged me with his positive point view to the every kind of event. I am so thankful to him due to the time and the efforts that he spent to improve my skills and thesis.

I am grateful to my co-supervisor Assoc. Prof. Dr. Atilla CİHANER for his assists while I was trying to achieve the goals of my thesis.

I am so thankful to Buket BEZGİN ÇARBAŞ for sharing her experiences in every step of my thesis studies.

I also would like to express my thanks to my friends at ‘Prof. Dr. Ahmet M. Önal Research Group’ and Merve İÇLİ ÖZKUT for their friendship and encouragement during my study.

I sincerely acknowledge my friends; Ejder BAŞARAN, Hana KASHT, Seval GÜNDÜZ, Dilek ÜNAL and Ceren UZUN with whom I had spent most of my time during thesis studies. I am appreciating the motivation that they provide for me.

I would like to extend my gratitude to my family for every single thing. Their supports are invaluable.

Finally, I want to thank to METU-Chemistry Department.

TABLE OF CONTENTS

ABSTRACT	iv
ÖZ	v
ACKNOWLEDGEMENTS	vii
TABLE OF CONTENTS	viii
LIST OF FIGURES	xi
LIST OF TABLES	xiii
LIST OF ABBREVIATIONS	xiv
CHAPTERS	1
1. INTRODUCTION	1
1.1. Brief History	1
1.2. Polymerization Techniques for CPs	2
1.2.1. Electrochemical Polymerization	2
1.2.2. Chemical Polymerization	5
1.2.3. Band Theory	6
1.3. The Conductivity of CPs	7
1.3.1 Doping Process	9
1.4 Polyfluorenes	10
1.4.1. General Point of View for Polyfluorenes	10
1.4.2. Synthesis of PFs	12
1.4.2.1. Functionalization of Fluorene Ring	13
1.4.3. Copolymers of PFs	14
1.5. Polyfurans	15
1.5.1. General Point of View for Polyfurans	15
1.5.2. Synthesis of PFus	16
1.6. Furan-Fluorene Based Copolymers	18
1.7. Electrochromic Properties	19
1.7.1. Contrast Ratio	19
1.7.2. Coloration Efficiency	19
1.7.3. Switching Time	19

1.8. Application of CPs.....	20
1.9. Motivation.....	20
2. EXPERIMENTAL	22
2.1 General Information.....	22
2.2. Procedure.....	23
2.2.1. Monomer Synthesis.....	23
2.2.1.1. Synthesis of FOF.....	24
2.2.1.2. Synthesis of FFF	24
2.2.1.3. Synthesis of FHF.....	24
2.2.2. Polymer Synthesis.....	25
2.2.2.1. Electrochemical Polymerization of Monomers.....	25
2.3. Characterization of Polymers.....	26
2.3.1. Cyclic Voltammetry (CV).....	26
2.4. Spectroelectrochemistry	27
2.5. Kinetic Properties.....	28
3. RESULTS AND DISCUSSION	29
3.1. Electrochemical Properties of Monomers.....	29
3.1.1. Cyclic Voltammograms of Monomers.....	29
3.1.2. Electropolymerization of Monomers	32
3.2. Characterization of Polymers.....	34
3.2.1. FTIR Spectroscopy	34
3.2.2. Thermal Gravimetric Analysis (TGA).....	36
3.3. Electrochemical Properties of Polymers	38
3.4. Stability of Polymer Films	40
3.5. Spectroelectrochemical Properties of Polymers.....	42
3.6. Kinetic Properties of Polymers	45
3.7. Chemical Polymerization of FHF.....	48
4. CONCLUSIONS	51
REFERENCES.....	52
APPENDICES	59

A. NUCLEAR MAGNETIC RESONANCE SPECTRA OF PFOF, PFFF and PFHF MONOMERS	59
B. FTIR SPECTRA OF OUT-COMING GASES DURING TGA FOR POLYMERS; PFOF, PFFF AND PFHF.....	62
C. FTIR SPECTRA OF FHF AND PFHF.....	65

LIST OF FIGURES

FIGURES

Figure 1. Repeating units of some common conducting polymers.	2
Figure 2. Polymerization mechanism of heterocyclic monomers via electrochemical techniques (X = S, O, NH) [27]..	4
Figure 3. Possible α - α' and α - β couplings of unsubstituted heterocyclic monomers (X = S, O, NH) [27].....	5
Figure 4. Chemical polymerization routes for furan based monomers.	5
Figure 5. Simple diagram for explaining the band theory [35].....	6
Figure 6. Effect of polymerization on band gap in thiophene [36].....	7
Figure 7. Charge carrier formations in polythiophene.	8
Figure 8. Formation of polaron and bipolaron states, bipolaron bands and metallic-like states during doping of conjugated polymers.....	9
Figure 9. (A) Chemical dopings (n-type and p-type). B) Electrochemical dopings (n-type and p-type) [41].	10
Figure 10. Some copolymers of PFs.	11
Figure 11. Some PFs covering whole visible spectrum.	12
Figure 12. RF naming system (R: alkyl groups).	13
Figure 13. Substitution of fluorene ring with carbonyl group.....	13
Figure 14. Substitution of fluorene ring with alkyl chains.....	14
Figure 15. Band gaps for some fluorene based copolymers [54].....	15
Figure 16. Reaction of PFu with water.	17
Figure 17. Electropolymerization mechanism for furan.	18
Figure 18. Synthesis of monomers; a) FOF, b) FFF and c) FHF.	23
Figure 19. CV waveform.....	26
Figure 20. CV for a reversible anodic oxidation and reduction process.	26
Figure 21. Cyclic voltammograms of FOF, FFF and FHF in 0.1 M TBAH/DCM solution at 100 mV/s vs. Ag/AgCl. Concentration of monomers: FOF= 4.0×10^{-3} M, FFF= 6.0×10^{-3} M, FHF= 8.0×10^{-3} M.	30

Figure 22. Cyclic voltammograms of (a) FOF, furan and fluorenone. (b) FFF, furan and fluorene (c) FHF, furan and 2, 7-dibromo-(9, 9) dihexylfluorene, respectively. In 0.1 M TBAH/ACN solution at 100 mV/s vs. Ag/AgCl. Concentration of monomers: Furan= 2.0×10^{-3} M, Fluorenone= 6.0×10^{-3} M, FOF= 4.0×10^{-3} M Fluorene= 2.0×10^{-3} M, FFF= 4.0×10^{-3} M, 2,7-dibromo-(9,9)dihexylfluorene= 16.0×10^{-3} M, FHF= 8.0×10^{-3} M.	31
Figure 23. Electropolymerization of 4.0×10^{-3} M of FOF in DCM/ACN (3/97;v/v), 6.0×10^{-3} M of FFF in DCM and 14.0×10^{-3} M of FHF in ACN with 0.1 M TBAH at 100 mV/s (vs. Ag/AgCl).	33
Figure 24. FTIR spectrums for monomers and their polymers.	35
Figure 25. Thermograms for a) FOF, b) FFF and c) FHF.....	37
Figure 26. Scan rate dependence of polymer films on a Pt disk electrode in 0.1 M TBAH/ACN and relationship of anodic (ip,a) and cathodic (ip,c) current peaks as a function of scan rate between neutral and oxidized states of (a) PFOF film (b)PFFF film (c)PFHF film in 0.1 M TBAH/ACN (vs.Ag/AgCl)	39
Figure 27. Stability test for PFOF, PFFF and PFHF films in 0.1 M TBAH/ACN as a scan rate of 60 mVs-1, 80 mVs-1, 100 mvs-1 respectively under nitrogen atmosphere by CV as a function of : A: 1st; B: 200th; C: 400th; D: 600th; E: 800th, F: 1000th cycles.....	41
Figure 28. Optical absorption spectra of PFOF, PFFF and PFHF on ITO electrode in 0.1 M TBAH/DCM at potential range between -0.20 and 1.20 V.	44
Figure 29. Chronoabsortometry experiments for (a) PFOF film switched between 0.0 V and 1.15 V (b) PFFF film switched between 0.0V and 1.20 V (c) PFHF film switched between 0.0 V and 1.20 V with an interval time of 10 s on ITO in 0.1 M TBAH/ACN vs. Ag wire.....	47
Figure 30. Bromination of FHF.	49
Figure 31. Chemical polymerization of FHF via Yamamoto coupling.....	50

LIST OF TABLES

TABLES

Table 1. Colors of the PFOF, PFFF and PFHF on ITO electrodes in their neutral and oxidized state.....	45
Table 2. Optical and electrochemical properties of PFOF, PFFF and PFHF.....	48

LIST OF ABBREVIATIONS

ACN	Acetonitrile
CB	Conduction Band
CP	Conjugated Polymer
CE	Coloration Efficiency
CV	Cyclic Voltammetry
DAD	Donor Acceptor Donor
DCM	Dichloromethane
FFF	2-(2-(furan-2-yl)-9H-fluoren-7-yl) furan
FHF	2-(2-(furan-2-yl)-9, 9-dihexyl-9H-fluoren-7-yl)furan
FOF	2, 7-di (furan-2-yl)-9H-fluoren-9-one
FTIR	Fourier Transform Infrared Spectroscopy
HOMO	Highest Occupied Molecular Orbital
ITO	Indium-tin oxide
LUMO	Lowest Unoccupied Molecular Orbital
NMR	Nuclear Magnetic Resonance
PF	Polyfluorene
Pt	Platinum
PTh	Polythiophene
RE	Reference Electrode
rt	Room Temperature
SPEL	Spectroelectrochemical
TBAH	Tetrabutylammoniumhexafluorophosphate
THF	Tetrahydrofuran
VB	Valence Band
UV-VIS	Ultraviolet Visible
WE	Working Electrode
Δ%T	Percent Transmittance Changes

CHAPTER 1

INTRODUCTION

1.1. Brief History

Conducting polymers (CPs) are composed of conjugated polymer chains with delocalized π -electrons along the chain. History of CPs goes back to the doping process of polyacetylene. In 1970, H. Shirakawa discovered the formation of a shiny metallic film on the wall of the reaction vessel during the synthesis of polyacetylene with higher concentration of Ziegler-Natta catalyst. Then, H. Shirakawa collaborated with A. MacDiarmid and A. Heeger to investigate the properties of this shiny material. The results of their collaborative work was published in the year 1977 and the three scientists were awarded by Nobel Prize in chemistry in 2000 for their invention that polyacetylene is very conductive when it is doped with iodine [1-5]. This successful work has been followed by a huge number of studies leading to discoveries of other CPs, such as polypyrroles [6], polythiophenes [7-9], polyfluorenes [10], polyanilines [11, 12], and polycarbazoles [13]. Their schematics are shown in Figure 1. The main aim of this further research was to overcome stability and processability problems of polyacetylene and to find application areas in the industry. Firstly, scientists hoped to use these materials instead of highly conducting metals for batteries and electrical transport. Nevertheless, doped states of these materials were not stable. This brought the hopes to more realistic line and CPs are started to be used as light-emitting diodes [14], electrochromic devices [15], organic solar cells [16], transistors [17], gas sensors [18] and electrochromic mirrors [19].

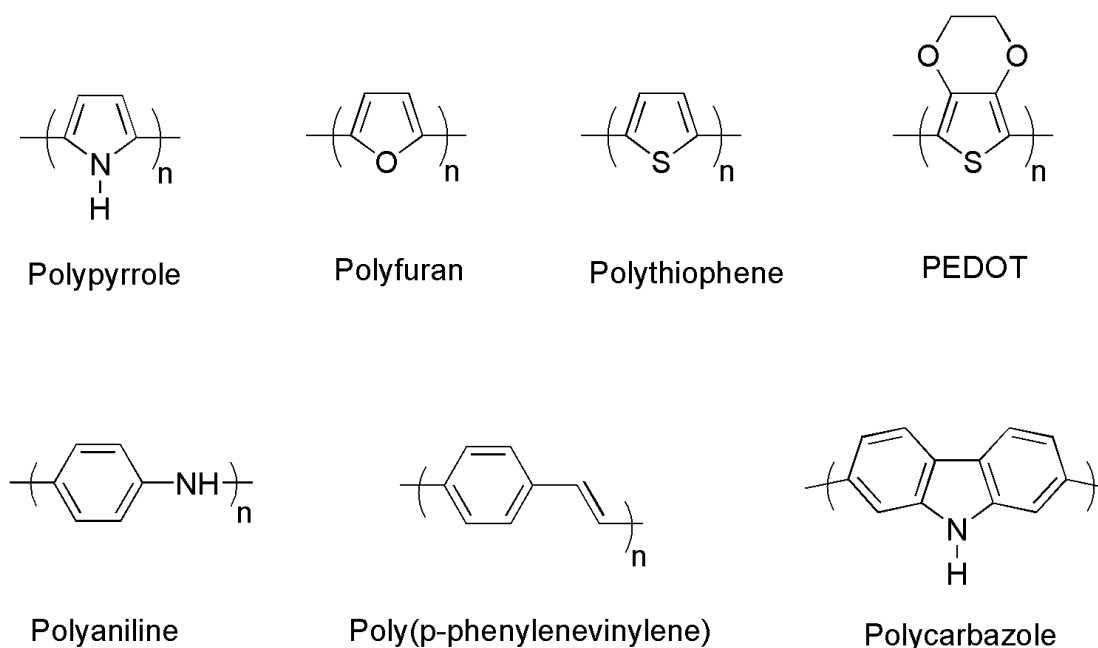


Figure 1. Repeating units of some common conducting polymers.

1.2. Polymerization Techniques for CPs

Generally, CPs can be synthesized by both chemical and electrochemical methods. Copolymerization, photochemical polymerization, metathesis polymerization, plasma polymerization, inclusion polymerization and solid state polymerization are the other types of polymerization techniques; however, they are not much preferable.

1.2.1. Electrochemical Polymerization

Electrochemical polymerization is a method in which monomer is either electro-oxidized or electro-reduced in a suitable reaction medium containing solvent and supporting electrolyte. Electrochemical polymerization is preferred in the synthesis of CPs due to its advantages over other types. These advantages are listed below; [20, 21]

- Monomers are used in very small amounts.
- Polymer film can be quickly coated on an electrode surface and can be directly utilized as a sensor or a battery.

- They provide in situ analysis to search the properties of CP and polymerization process by spectroscopic or electro analytical methods.
- Film thickness, conductivity and morphology can be controlled by adjusting applied voltage, scan rate and polymerization time.
- Contamination through side reactions can be prevented through the applied bias control.

Although electrochemical polymerization is quite simple, advantageous and selective, there are few points to take under consideration to obtain desired polymer with expected properties. For instance, in electrochemical polymerization selection of suitable solvent-electrolyte couple, electrodes, concentration of monomer and applied voltage get great importance because they have significant effects on the properties of the formed polymer [22]. In the case of solvent, dielectric constant and working potential window of the solvent are important. Dielectric constant must be high enough to dissolve monomer and electrolyte; however, it should not dissolve the polymer deposited on the electrode surface. Thus, any solvent that satisfies these criteria might be used provided that oxidation/reduction potential of the monomer is less than that of solvent-electrolyte couple. Concentration of the monomer is also important in synthesizing the expected amount of polymer on the electrode surface. In some cases polymerization might not take place if the concentration of the monomer is too low. On the other hand, electrolyte selection is also very important because it might affect the electrochemical properties of the polymer. To specify, electrolyte should be non-nucleophilic and inactive towards electrochemical reactions. Tetraalkylammonium tetrafluoroborate, tetraalkylammonium perchlorate, tetraalkylammonium hexafluorophosphate and lithium perchlorate are some of the most popular electrolytes [23]. Finally, applied potential range should be as small as possible to have limited amount of side reactions. The highest potential applied in the synthesis must be the potential that is exactly equal to the oxidation potential of the monomer. Otherwise, overoxidation might occur [24]. During the electrochemical polymerization, monomers are oxidized to form reactive radical cations as

reaction intermediates. These radical cations can follow one of the two different routes to form polymer. They might couple with another neutral monomer and then they lose two protons to form a neutral dimer [25]. On the other hand, two different radical cations can also come together and form a neutral dimer by losing two protons [26]. Dimers also follow one of the same routes of synthesis as radical cations. Oxidation potential of dimer is lower than that of monomer due to increasing conjugation, so dimers are oxidized easier than monomers. As this process continues, polymer is coated on the working electrode surface with increasing number of repeating units. A general electro-oxidative polymerization mechanism for poly(heterocycles) is given in Figure 2.

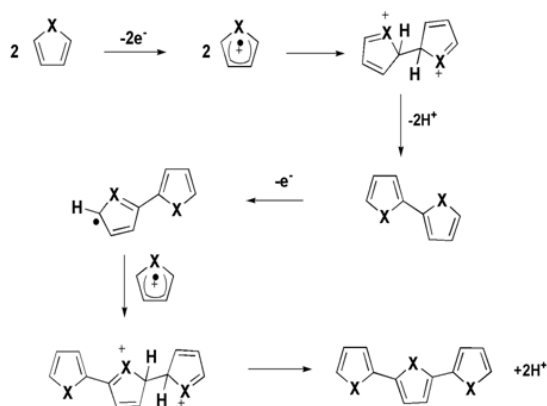


Figure 2. Polymerization mechanism of a heterocyclic monomer via electrochemical techniques ($X = S, O, NH$) [27].

During the electrochemical polymerization of poly(heterocycles) two different kinds of couplings, α - α' and α - β coupling, can take place (Figure 3). While α - α' coupling is the regular one, α - β coupling results in chain branching so, in polymer structure different parts with different conductivity and electronic properties occur. As predictably, homogeneous structure of the polymer is harmed by α - β coupling and this is avoided, usually, by replacing β and β' hydrogen atoms with suitable functional groups.

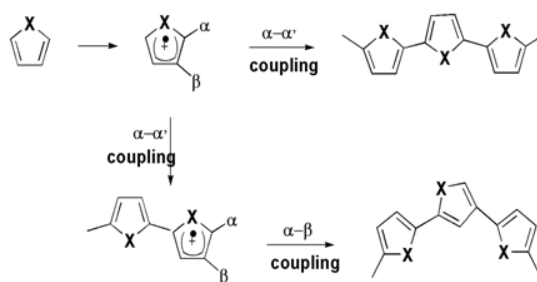


Figure 3. Possible α - α' and α - β couplings of unsubstituted heterocyclic monomer (X = S, O, NH) [27].

1.2.2. Chemical Polymerization

Chemical polymerization is the most widely used synthesis method to produce CPs since it is the simplest and the least expensive technique [28, 29]. Chemical polymerization can be achieved either by oxidative polymerization or transition-metal mediated polymerization. In oxidative chemical polymerization, conducting (doped) form of the polymer can be obtained using oxidizing agents. Anhydrous ferric chloride, FeCl_3 , is the most widely used oxidizing agent for poly(heterocycles) [29, 30]. However, other oxidizing agents are also present [29, 31]. Since neutral form is more stable for most CPs, they are reduced with reducing agents such as hydrazine and ammonium hydroxide if they are obtained in the oxidized form during chemical polymerization. However, if strong oxidizing agents are used in the polymerization, some undesired reactions like decomposition, overoxidation and ring opening might happen [32]. Moreover, catalytic Grignard method is also used for the polymerization of pyrrole, furan and thiophene based monomers [33]. The main reason for preferring catalytic Grignard technique is that it is possible to eliminate undesired couplings in this method.

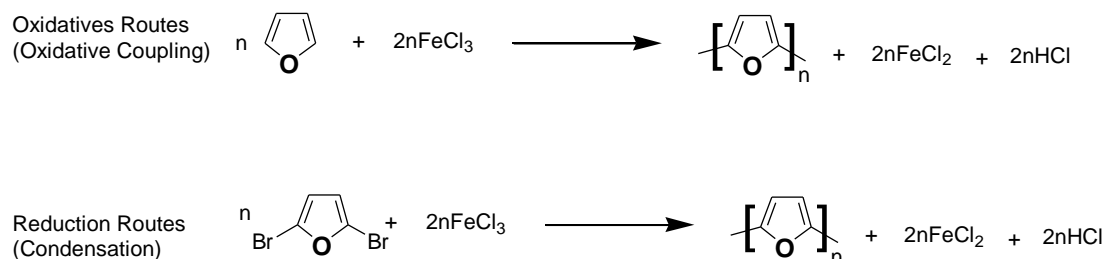


Figure 4. Chemical polymerization routes for furan based monomers.

1.2.3. Band Theory

Materials are classified according to their electrical conductivities as conductors, semiconductors and insulators. CPs belong to semiconductor group and band model is used to define the conductivity of CPs (semiconductors). In this theory, electrical properties of materials are explained on the basis of energy difference between the highest occupied molecular orbital (HOMO) and the lowest unoccupied molecular orbital (LUMO), which is called as the band gap [34].

In metals, valence band and conduction band form a single band by overlapping. Thus, their band gaps are zero and conductivity is achieved by the movement of electrons between partially filled bands. Moreover, in insulators, band gap is greater than 3.0 eV and electron movement from valence band to conduction band is not possible. On the other hand, semiconductors have band gaps between the metals and insulator (Figure 5).

In intrinsic semiconductors, electrons occupying the valence band and the conduction band is empty and there exist no other energy states between valence and conduction bands. Upon excitation via photochemical or thermal ways, electrons in the valence band are promoted to the conduction band which creates vacancies for the free movement of electrons both in the conduction and valence band [35].

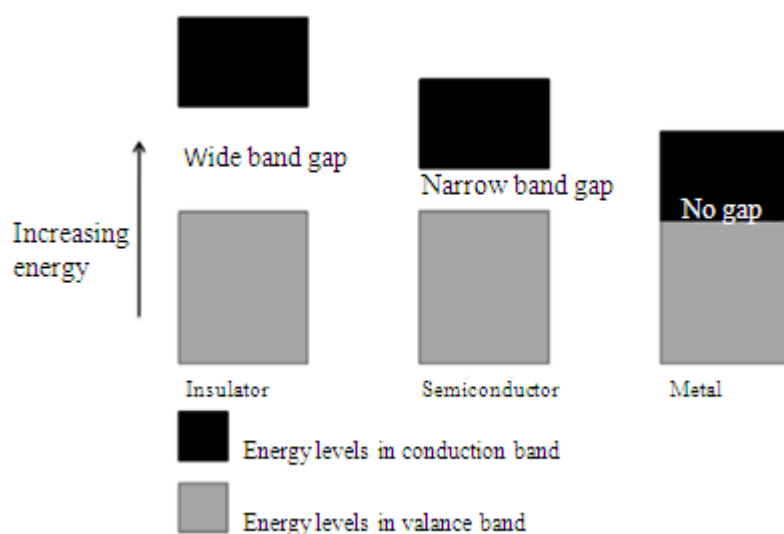


Figure 5. Simple diagram for explaining the band theory [35].

Figure 6 depicts the formation of valance and conduction bands as the thiophene goes to polythiophene via polymerization with increasing conjugation. As the number of thiophene units increases, the number of π bonding and π antibonding orbitals also increases. As a consequence of this increase, the energy levels become closely spaced and they form bands. The highest energy filled band, which is analogous to HOMO and consists of filled bonding π orbitals, is called the valence band. The next higher band, which is analogous to the LUMO and composed of antibonding π^* orbitals, is called the conduction band. As predictably, as the degree of polymerization increases, energy difference between HOMO and LUMO levels decreases.

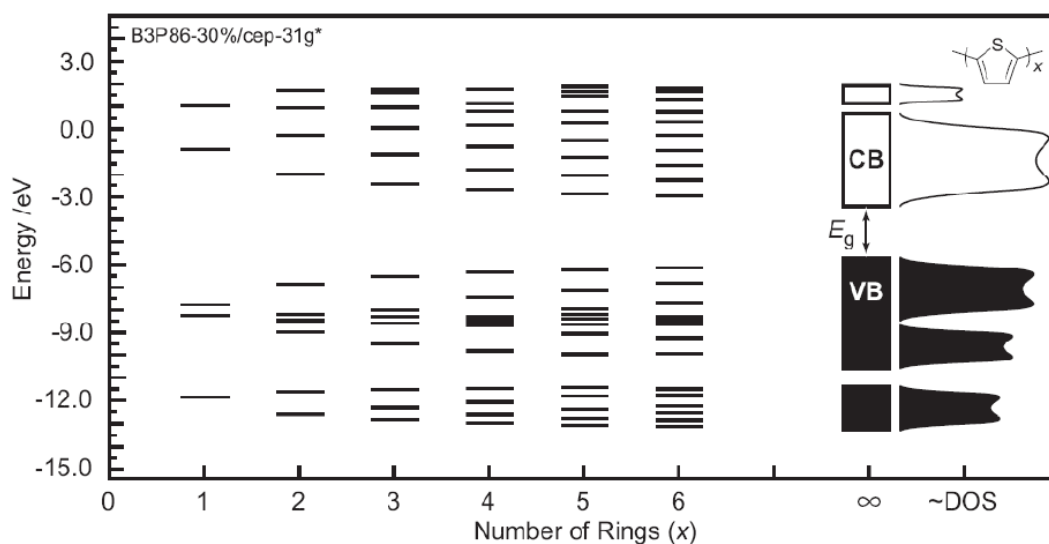


Figure 6. Effect of polymerization on the band gap in thiophene [36].

1.3. The Conductivity of CPs

Conduction mechanism in CPs is basically defined as the motion of negative or positive charge carriers along π orbitals through the polymer. Charge carriers can be defined as defects that occur during the oxidation or reduction process of the polymer. Positive charge carriers (p-type) are produced by oxidation of the polymer, while negative charge carriers (n-type) are created by reduction. The formation of p-type and n-type charge carriers lowers the band gap of the polymer.

During the oxidation process of a polymer (Figure 7a), electrons are removed from HOMO level so the radical cations (polarons) are created (Figure 7b). The radical cations move through some specific parts of the chain and this movement is accompanied by the motion of counter ions through the polymer to maintain neutrality. Further oxidation in the same chain results in the formation of bipolarons (Figure 7c). When polymer is highly doped, the energy levels overlap to form a narrow gap resulting in a decrease in the band gap and an increase in the conductivity (Figure 8). The same process also occurs during the reduction of polymer (n-doping) [37].

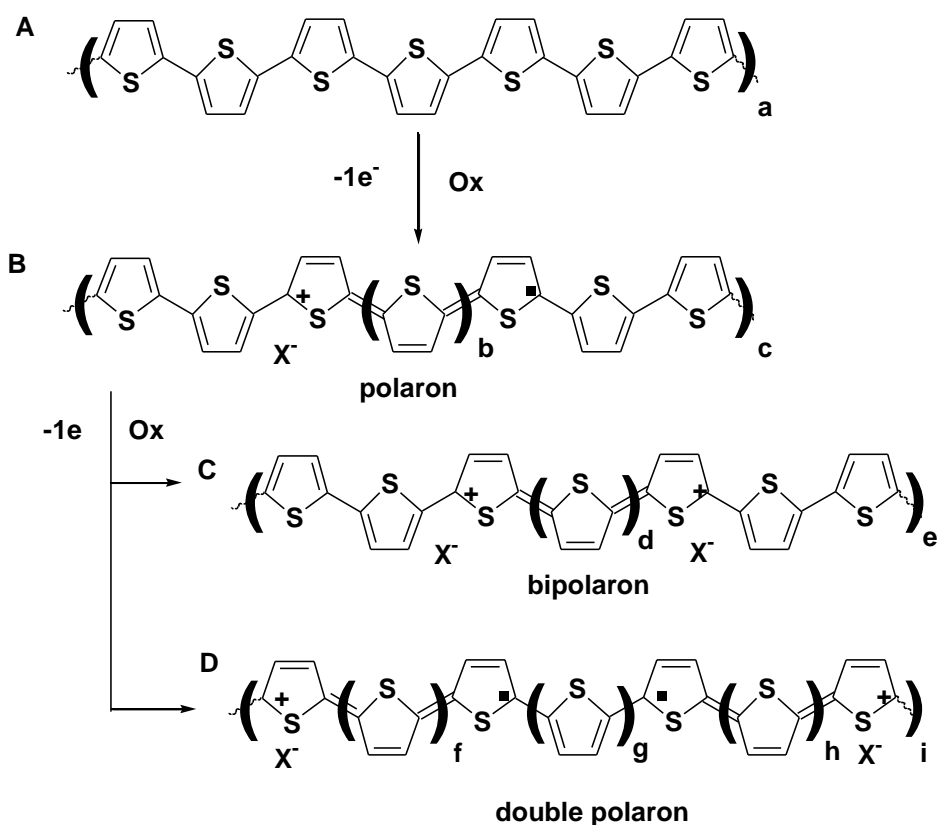


Figure 7. Charge carrier formations in polythiophene.

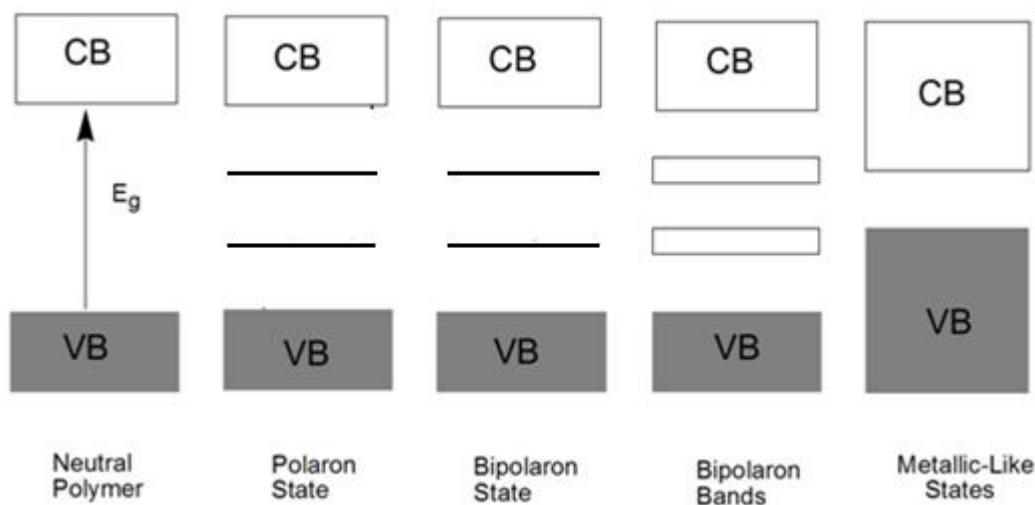


Figure 8. Formation of polaron and bipolaron states, bipolaron bands and metallic-like states during doping of conjugated polymers.

1.3.1 Doping Process

Doping is the name of the reversible process that describes the formation of the charge carriers on the polymer backbone. Charge carriers are created by the addition or removal of electrons to the structure as stated earlier. It is a very significant process since it provides the adjustment of the electrical conductivity of the polymer. In other words, it is possible to put a polymer in any form between insulator to highly conductive material by simply adjusting the doping level. There are two types of doping process; chemical doping and electrochemical doping. Figure 9 illustrates these two types of doping.

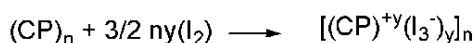
Although chemical doping is straightforward and effective method, it is not easy to control the level of doping in this process. It generally results in heterogeneous doping instead of complete doping. Electrochemical doping has been investigated to handle the matter [38].

Electrochemical doping is superior to chemical one due to the fact that it is controllable by just potential adjustments [39]. In electrochemical process, a polymer

can be reduced or oxidized forming charge, which will be neutralized by counter ion coming from the electrolyte, on the chain [40].

(A) Chemical Doping

(a) p-type doping



(b) n-type doping



(B) Electrochemical Doping

(a) p-type doping



(b) n-type doping

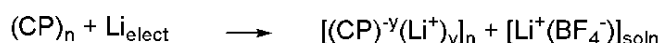


Figure 9. (A) Chemical dopings (n-type and p-type). (B) Electrochemical dopings (n-type and p-type) [41].

1.4. Polyfluorenes

1.4.1. General Point of View for Polyfluorenes

Among CPs, polyfluorenes, PFs, are of great interest because they have high photoluminescence efficiency, high hole mobility and good photostability. They emit blue light with photoluminescence efficiency of 50 % in the solid form and 80 % in the solution [42, 43]. They are promising electroluminescent materials and used in organic light emitting diodes. However, they have some limitations such as they have high energy barriers for hole injection and poor solubility in organic solvents. On the other hand, during the synthesis it is quite easy to substitute various functional groups from C-9 position to add desired properties to the structure like solubility in common organic solvents [44, 45]. Branching of biphenyl structure at the C-9

position also results in planarity which enhances the conjugation; thus, lowers the band gap.

Several random and alternating copolymers (Figure 10) have been synthesized to increase device efficiency and suppress the low energy emission. However, addition of different monomers to the polymer backbone affected stiffness and liquid crystalline properties of PFs [46].

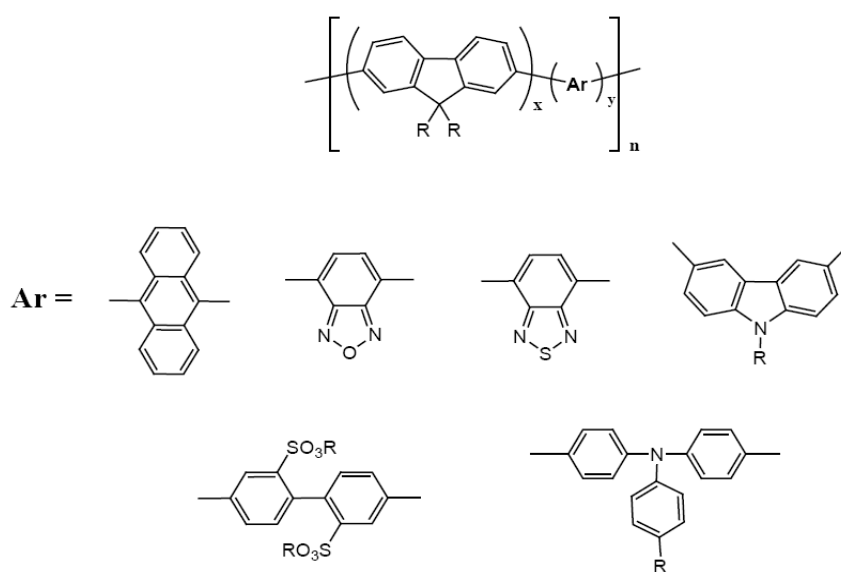


Figure 10. Some copolymers of PFs.

On the other hand, it has been proven that if the right comonomer couple can be chosen, PF family provides correct hole and electron-transport properties and color control. In literature, different copolymers of PFs are found with light emitting properties covering hole visible spectrum (Figure 11) [47].

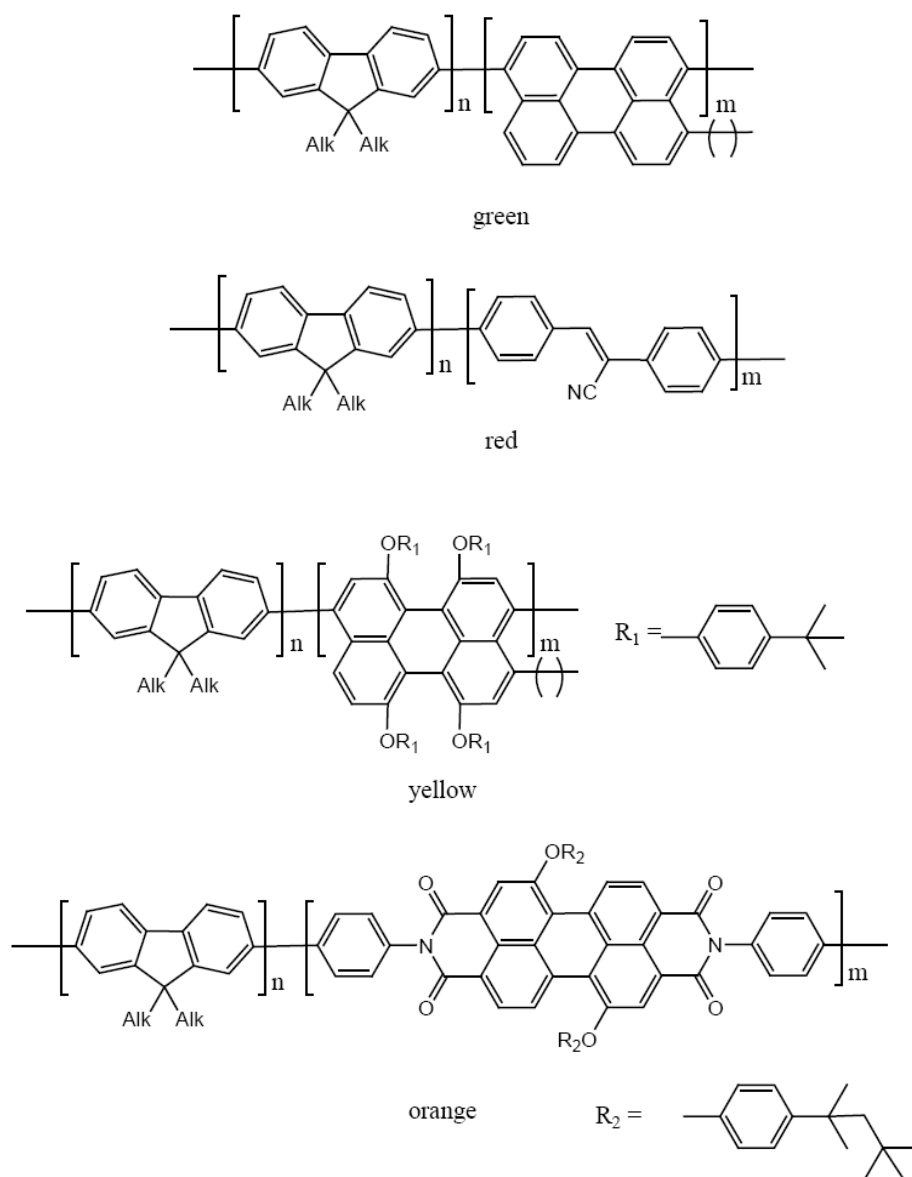


Figure 11. Some PFs covering whole visible spectrum.

1.4.2. Synthesis of PFs

PFs are promising blue light emitting CPs; therefore, various synthesis procedures have been developed so far. PFs are generally functionalized from 9 positions and Figure 12 shows the details about naming system of PFs.

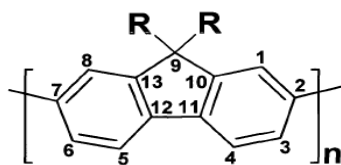


Figure 12. PF naming system (R: alkyl groups).

Fukuda's group was first to synthesize PF [48, 49]. The aim of the group's study was to synthesize a heat stable and fusible CPs. Fukuda et al. polymerized fluorene using oxidative coupling method. The group polymerized fluorene with oxidizing agent FeCl_3 . Although they were not able to achieve the goals of the study, they have invented a new class of light emitting polymer. Products obtained upon oxidative coupling were lack of quality. They were low in molecular weight and there were traces of crosslinking during polymerization. Therefore, other methods were preferred to be used such as Suzuki coupling and Stille coupling.

1.4.2.1. Functionalization of Fluorene Ring

Fluorene can easily be functionalized from C-9 bridging position to obtain desired properties. Fluorene has been substituted with carbonyl functional group by Ranger et al. for the first time (Figure 13) [24]. Actually, fluorene that is substituted with carbonyl functional group has a special name; fluorenone [50].

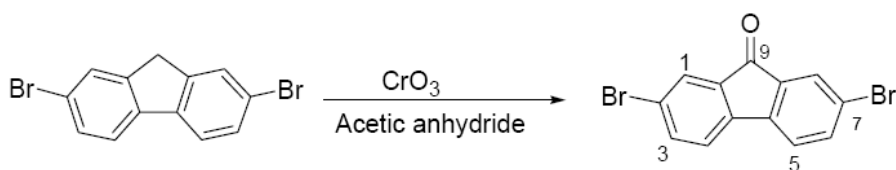


Figure 13. Substitution of fluorene ring with carbonyl group.

In addition, fluorene can be functionalized by alkyl groups to obtain soluble and processible CP (Figure 14) [51].

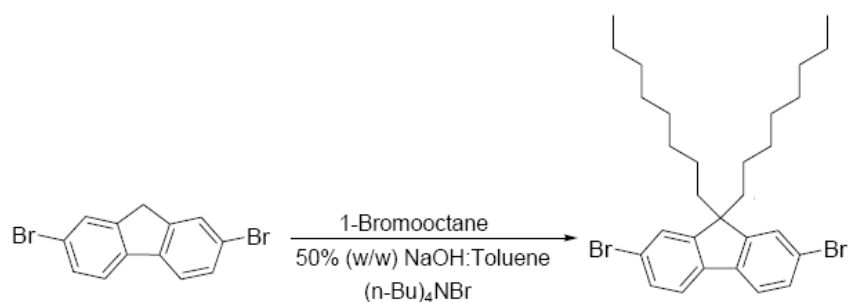


Figure 14. Substitution of fluorene ring with alkyl chains.

1.4.3. Copolymers of PFs

Copolymerization of PFs with different aromatic monomers can be performed by Stille Coupling procedure. To perform Stille Coupling reactions, fluorene monomer needs to be brominated and Z. Yacob has brominated fluorene ring for the first time [52]. In addition, copolymerization of PFs with other kind of aromatic molecules has been performed to obtain various colored materials by changing the band gap energy (Figure 15). The synthesis of alternating copolymers of PFs which can also be named as donor-acceptor-donor (DAD) systems have been done for this purpose [53]. Previously, different copolymers of fluorene unit have been synthesized in our research group (Figure 15) that copolymerization is an efficient method for the band gap control.

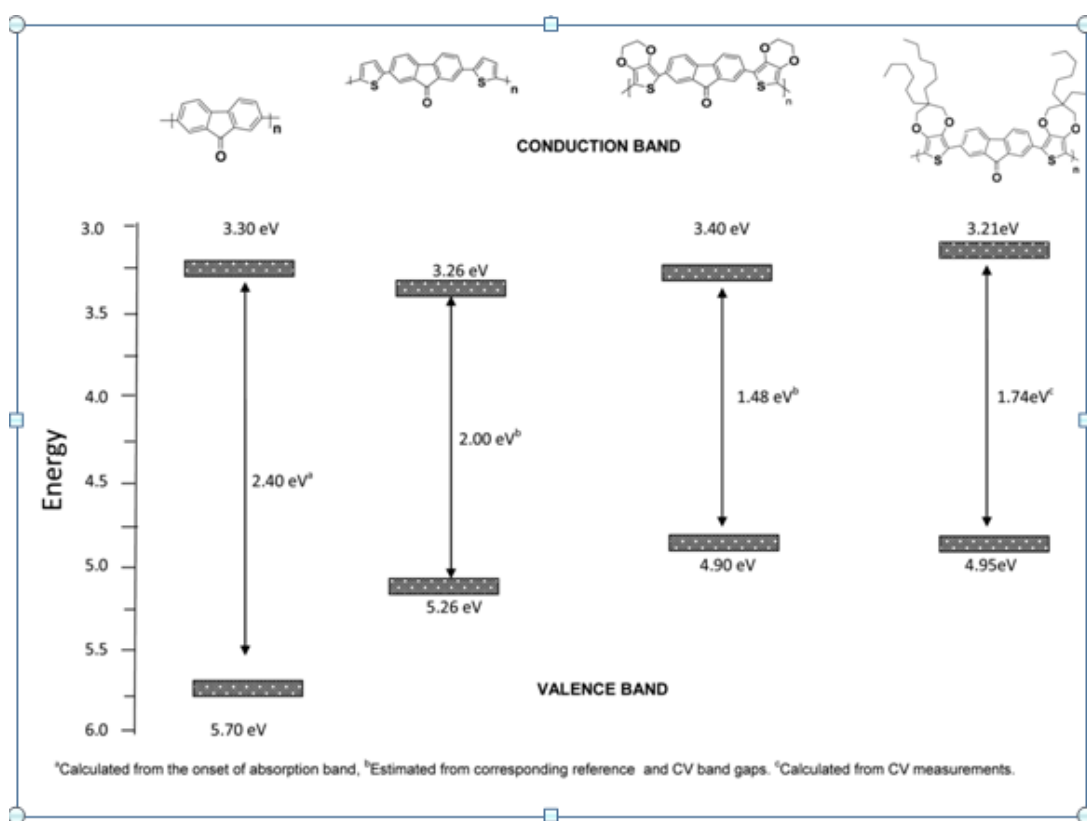


Figure 15. Band gaps for some fluorene based copolymers [54].

1.5. Polyfurans

1.5.1. General Point of View for Polyfurans

Furan is one of the five membered heterocyclic monomers like pyrrole and thiophene that include nitrogen or sulphur instead of oxygen atom, respectively. Since polyfuran (PFu) has a conjugation of electrons among the π orbitals, it has been topic for many detailed CP studies. However, studies on PFu are very limited when compared to polypyrrole and polythiophene due to the difficulties in the synthesis, resulting from lower aromaticity of furan ring. PFu synthesis via electrochemical techniques was reported by Tournillon and Garnier for the first time [55] and then Ohsawa et al. synthesized PFu films by electrochemical methods [56]. Electrical conductivity of PFu was found to be lower than both polypyrrole and polythiophene due to the fact that PFu does not have conjugated chains as long as polypyrrole or polythiophene. Glenis et al. also synthesized PFu films; however, they used terfuran

in the study to perform the synthesis at lower potentials [57]. Nessakh et al. investigated electrochemical properties of furan via cyclic voltammetry (CV); however, they were not able to obtain PFu [58]. The first conjugated PFu synthesis has been achieved by Zotti et al. by performing reductive coupling of 2,5-dibromofuran with the help of the catalyst; $\text{Ni}(\text{bipy})_3^{2+}$ and also PFu was coated on ITO electrode surface to observe electronic absorption spectrum [59]. They also tried to synthesize PFu via electrochemical oxidation. Their research resulted in a product with low conjugation due to the acid catalyst used. Carrillo et al. reported that they have achieved the synthesis of black PFu films via perchlorate doping; however, there were evidences for furan ring opening [60]. Our research group was able to synthesize conducting PFu films via potential cycling utilizing tetrabutylammonium perchlorate and sodium perchlorate as electrolyte with some amount of ring opening during the oxidation of the furan [61]. Boron trifluoride (BF_3) – ethyl ether (EE) solvent mixture was used to synthesize PFu films by Wan et al. and this resulted in less ring rupture than earlier studies [62]. Finally, in the year 2006, our research group synthesized conjugated PFu films successfully in acetonitrile (ACN)/ BF_3 /EE solvent system without any ring rupture [63]. In this study, PFu film was used in electrochromic device application and it was concluded that if convenient polymerization medium is used, PFu films can also be a promising candidate in some applications as the other five membered heterocyclic analogues. As can also be understood from above citations, PFu synthesis is a really challenging process.

1.5.2. Synthesis of PFus

As other types of CPs, PFu synthesis can be performed by repetitive cycling, constant potential and constant current electrolysis. The weaker side of PFu is the ring rupture when nucleophiles attack to the ring. This is the reason for using aprotic solvents that are poor nucleophiles or solvent mixtures like BF_3 /EE; EE is added to the medium to reduce the acidic effect of BF_3 in the PFu synthesis. Furthermore, during PFu synthesis, reaction medium can not be an aqueous solution since furan ring undergoes ring opening process upon reaction with water (Figure 16) [64].

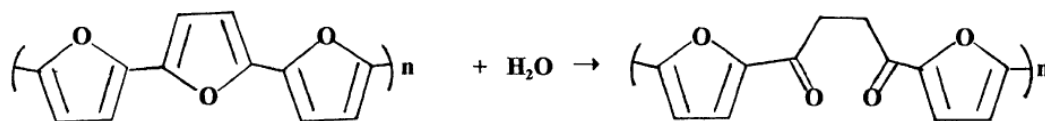


Figure 16. Reaction of PFu with water.

In electrolyte selection, solubility, nucleophilicity and degree of dissociation in a proper solvent are the most significant features to be a reason for choice. Tetraalkylammonium salts are providing all the desired properties; their solubility and degree of dissociation are higher while their nucleophilicity is lower. Therefore, they are used as electrolytes in PFu synthesis [65-68]. In addition, concentration of monomer is another important variable because the concentration of the monomer increases with the electroactivity of polymer film [69, 70]. In literature, a few different polymerization mechanisms have been proposed for the polymerization of pyrrole; although, Diaz's mechanism is considered to be the right one [71, 72]. On the other hand, the polymerization mechanism proposed by Diaz considered to be also valid for furan polymerization (Figure 17). According to Diaz mechanism, the presence of water causes the completion of polymerization (Figure 17(g)) [73].

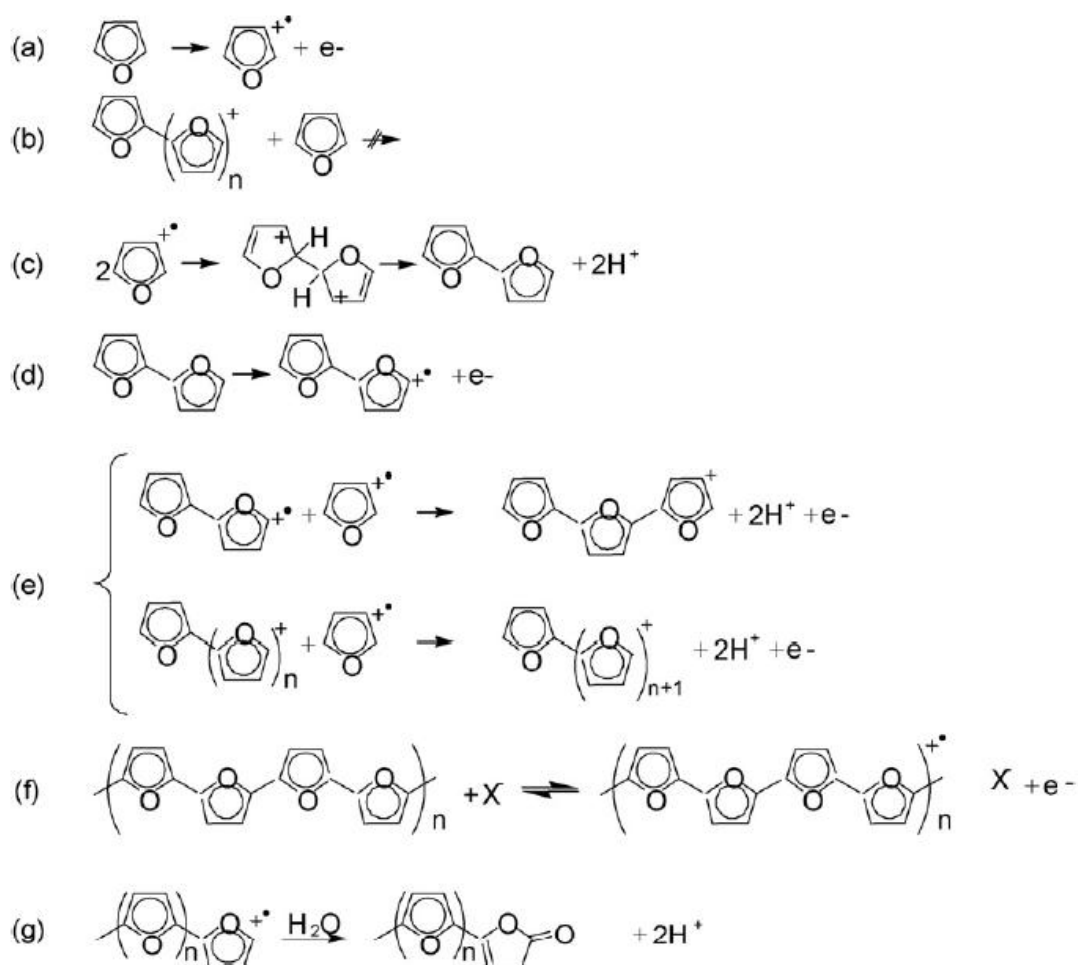


Figure 17. Electropolymerization mechanism for furan.

1.6. Furan-Fluorene Based Copolymers

PFs and copolymers of PFs that have been synthesized with different heterocycles are promising materials for organic electronics; therefore, they have been investigated frequently [74-77]. Copolymers that include fluorene, bearing and electron withdrawing group, and other conjugated heterocyclics is necessary for creating DAD systems that provide band gap control in electrochromic device applications [78]. Different donor units might be added to the fluorene unit to obtain DAD systems. In addition, it is quite easy to functionalize acceptor fluorene unit with different groups to observe the effects of the substituents on the properties of DAD

system. To illustrate, it is possible to improve solubility and stability of DAD system via substituting fluorene unit with alkyl groups from C-9 bridging position.

1.7 Electrochromic Properties

1.7.1 Contrast Ratio

Contrast ratio or percent transmittance is the percent transmittance difference between the colored and the bleached states. Percent transmittance of a material is calculated by subtracting transmittance in reduced state from the transmittance in oxidized state ($\Delta\%T = T_{ox} - T_{red}$). Percent transmittance of a material at different wavelengths is not the same; so that, a wavelength has to be selected for the calculations [79]. As expected, a wavelength with highest transmittance is used in the analysis.

1.7.2. Coloration Efficiency

Electrochromic materials change color upon external potential applications and coloration efficiency is the measure of that color changing ability. CE is calculated from the equations below;

$$CE = \Delta OD(\lambda) / Q_d \quad (1-1)$$

$$\Delta OD = \log [T_{ox}/T_{red}] \quad (1-2)$$

$$Q_d = Q / A \quad (1-3)$$

In above equations, ΔOD is optical density change at a certain wavelength, Q_d is the charge and A is the area of the electrode [80, 81]. If coloration efficiency equation is examined, it is clear that charge should be low while the change in transmittance must be high to have high coloration efficiency.

1.7.3 Switching Time

Switching time (t_s) is the time necessary for an electrochromic material to change its color during the redox process, i.e. transition from fully oxidized state to fully reduced state or vice versa. In electrochromic devices, very short switching times are

preferable while it is not necessary to have that much short switching times in some other applications such as rear-view mirrors, windows, etc.

1.8. Applications of CPs

CPs have a wide range of application areas due to the facilities in processing and cost. In addition, CPs are much more advantageous than other materials because it is easier to functionalize CPs to add desired properties. Application areas of CPs can be divided into three main categories according to the form of the CP during the application. In the first group, CPs are used in neutral form by getting use of luminescent and semiconductor properties. Transistors [82] and Organic Light Emitting Diodes (OLEDs) [83] are the specific examples for the category. In the second group, CPs are used in applications in the conducting form. Capacitors [84, 85], enzyme immobilization [84-86] and photographic film applications [87] are among the application areas of this group. Finally, third group applications mainly depend on the reversible switching ability of the CPs between the reduced and oxidized forms. Upon these reversible cycles, CPs change color and also their conductivities differ from one form to another. Electrochromic materials [88-91], sensors [92], actuators [93] and drug delivery [94] are among the application areas whose working principles depend on reversible switching ability.

1.9. Motivation

In literature, there are two popular ways to enhance optical properties of fluorenes. The first route is to functionalize fluorene from C-9 position and the second one is to copolymerize fluorene with other aromatic substances. In this study, these two ways have been combined by creating copolymers of differently substituted fluorenes with furan units to create DAD systems. For all three monomers, donor unit was chosen to be furan ring since it can add desired properties to the DAD systems as thiophene and pyrrole analogues. In addition, there are very limited number of studies about furan unit containing monomers due to the synthesis difficulties in the literature. Moreover, fluorene derivatives were the acceptor units and the effect of different substituents at C-9 position of fluorene unit was investigated. To illustrate, fluorene

was substituted with carbonyl group to search the effect of electron withdrawing group and also it was substituted with hexyl groups to enhance the solubility of the resulting polymer. Investigating the properties of the newly designed DAD systems was the main aim of the study.

CHAPTER 2

EXPERIMENTAL

2.1 General Information

All chemicals were purchased from Sigma Aldrich and used as received except for the solvents; acetonitrile and dichloromethane. Solvents were distilled over CaH_2 under N_2 atmosphere before using in the experiments. Solvents were used as electrolyte solution containing tetrabutylammonium hexafluorophosphate (TBAH) as the electrolyte. Ag/AgCl in 3 M NaCl (aq) solution was used as a reference electrode while a platinum disc (0.02 cm^2) was working electrode and platinum wire was the counter electrode. Polymer films were synthesized via potential cycling and constant potential electrolysis techniques and electrochemical and optical behaviors of the resulting films were analyzed in solutions containing only electrolyte and solvent. Spectroelectrochemical properties of the polymer films were investigated on an indium tin oxide electrode (ITO, Delta Tech. 8–12 Ω , 0.7 cm x 5 cm) as a working electrode together with platinum wire as a counter electrode and Ag wire as a pseudo-reference reference. A Hewlett–Packard 8453A diode array spectrometer and a Gamry PCI4/300 potentiostat-galvanostat were used for in situ spectroelectrochemical studies and electroanalytical measurements, respectively. FTIR spectra were recorded on a Bruker Vertex 70 spectrophotometer equipped with attenuated total reflectance (ATR) unit. ^1H and ^{13}C NMR spectra were recorded on a Bruker NMR Spectrometer (DPX-400) in CDCl_3 using tetramethylsilane as the internal reference.

2.2. Procedure

2.2.1. Monomer Synthesis

All monomers; 2,7-di (furan-2-yl)-9H-fluoren-9-one (FOF), 2-(2-(furan-2-yl)-9H-fluoren-7-yl) furan (FFF) and 2-(2-(furan-2-yl)-9,9-dihexyl-9H-fluoren-7-yl)furan (FHF), were synthesized by the Stille Coupling [54] reactions of 2-(Tributylstannyl) furan with corresponding 2,7 brominated fluorene and its derivatives in the presence of Pd as the catalyst (Figure 18).

2-(Tributylstannyl) (2 equiv.), PdCl₂(PPh₃)₂ (0.02 equiv.) and corresponding 2,7-dibromofluorene derivative were placed in a 100.0 mL two-necked flask equipped with reflux condenser under N₂ atmosphere. Then, dry toluene was added as solvent and the reaction medium is heated till the reflux starts (100-110 °C). After stabilizing the temperature of the heater, the reactions have been stirred with magnetic stirrer for 7 days.

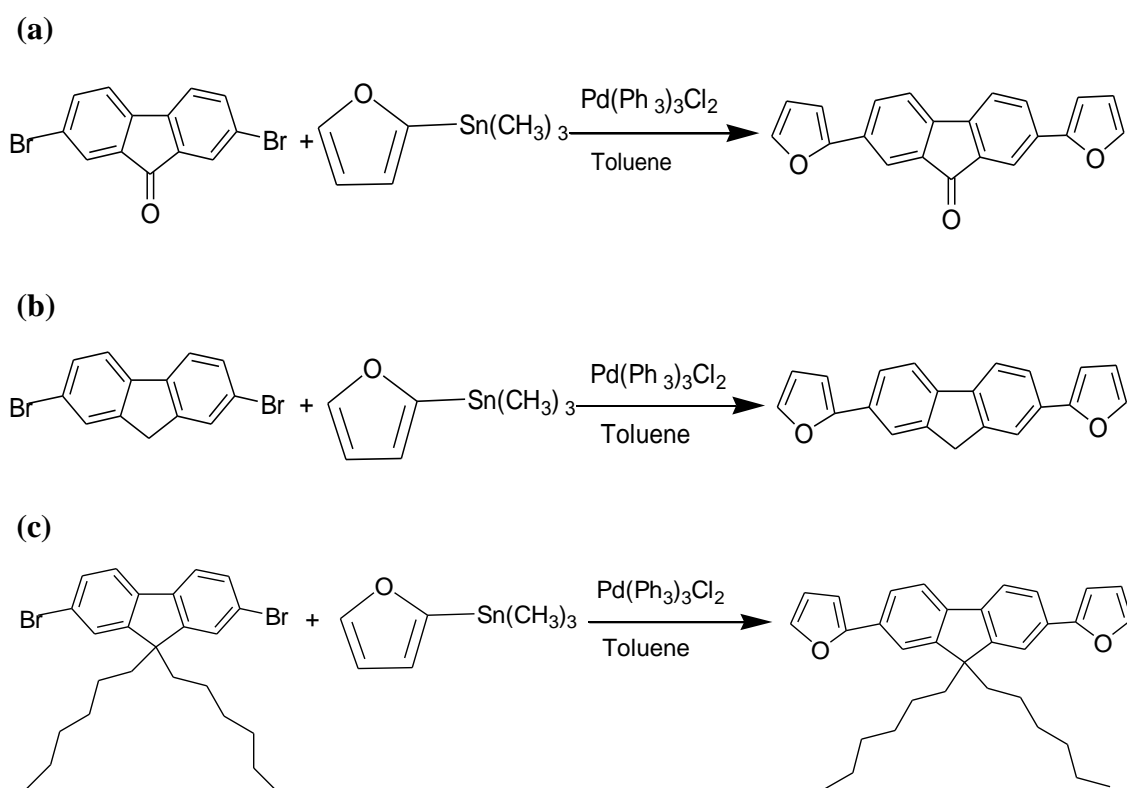


Figure 18. Synthesis of Monomers; a) FOF, b) FFF and c) FHF.

When the reaction was completed, solvent (toluene) was removed from the medium by distillation and product was separated from reaction side products with the help of column chromatography. Distilled hexane was used in column chromatography.

2.2.1.1. Synthesis of FOF

Reddish solid. Yield: % 70 ¹H NMR results of FOF: 7.914 (s, 2H), 7.784 (dd, J=7.6, J=1.6, 2H), 7.487 (m, 4H), 6.719 (d, J=3.2, 2H), 6.501 (m, 2H)

¹³C NMR results of FOF: 193.714, 152.902, 142.612, 142.550, 134.915, 131.612, 129.486, 120.607, 119.719, 111.915, 106.053

FT-IR results of FOF (ATR, cm⁻¹): 3122, 2960, 2922, 2854, 1709, 1598, 1452, 1376, 1290, 1266, 1175, 1140, 1071, 1009, 967, 910, 877, 780, 738, 690

HRMS: m/z: 313.0 [M⁺] (Calculated: 312.32)

Melting Point: 220 °C

2.2.1.2. Synthesis of FFF

Greyish white solid. Yield: %67 ¹H NMR results of FFF; 7.867 (s, 2H), 7.772 (d, J= 8,2H), 7.729 (d, J= 8.4, 2H), 7.502 (s, 2H), 6.698 (d, J= 3.6, 2H), 6.510 (m, 2H), 3.977 (s, 2H)¹³C NMR results of FFF; 154.41, 143.96, 141.96, 140.66, 129.47, 122.85, 120.35, 120.10, 111.77, 104.84, 36.96

FT-IR results of FFF (ATR, cm⁻¹): 3150, 3117, 3057, 2957, 2918, 2858, 1726, 1610, 1571, 1494, 1455, 1401, 1293, 1262, 1213, 1162, 1078, 1007, 928, 882, 828, 728, 670

HRMS: m/z: 298.1 [M⁺] (Calculated: 298.33)

Melting Point: 241 °C

2.2.1.3. Synthesis of FHF

Yellowish white solid. Yield: %60 ¹H NMR results of FHF; 7.709 – 7.673 (m, 4H), 7.652 (s, 2H), 7.521 (s, 2H), 6.727 (d, J=3.6, 2H), 6.527 (m, 2H), 2.035 (m, 4H), 1.146 – 0.993 (m, 12H), 0.787 (t, J= 6.8, 6H), 0.596 (m, 4H)

¹³C NMR results of FHF; 154.628, 151.439, 141.824, 140.107, 129.637, 122.825, 119.886, 117.979, 111.722, 104.777, 55.268, 40.509, 31.485, 29.705, 23.705, 22.568, 13.952

FT-IR results of FFF (ATR, cm⁻¹): 3117, 2921, 2854, 1597, 1530, 1497, 1458, 1413, 1374, 1285, 1252, 1218, 1157, 1134, 1078, 1012, 889, 821, 800, 726, 693, 642

Melting Point: 102 °C

2.2.2. Polymer Synthesis

2.2.2.1. Electrochemical Polymerization of Monomers

Electrochemical polymerization of FOF was performed on platinumium disc electrode via repetitive potential cycling between 0.00 V and 1.25 V at a scan rate of 100 mV/s. During the synthesis, 0.1 M TBAH was used as electrolyte while ACN and DCM mixture (3/97, v/v) was used as solvent. Since solubility of FOF is limited in ACN, little amount of DCM was used to dissolve the electrolyte and FOF. 6.0×10^{-3} M FOF was ideal for the polymerization. After the synthesis, polymer has been washed with ACN to remove unreacted FOF and electrolyte. Although polymerization of FFF was quite succesfull both in ACN and DCM, the later was preferred due to higher solubility of FFF in DCM. 0.1 M TBAH and DCM were the solvent electrolyte system for this polymerization. Repetitive cycling between 0.00 V – 1.25 V at a scan rate of 100 mV/s was used for the polymerization of FFF in DCM containing 6.0×10^{-3} M FFF and 0.1 M TBAH. PFFF was washed with DCM to remove unreacted monomer and electrolyte. As a difference from FOF and FFF, successful polymerization of FHF was only possible when ITO electrode was used. Since DCM was dissolving oligomers of FHF from the ITO surface, ACN was used as the solvent for the reaction while 0.1 M TBAH was electrolyte. The ideal conditions for obtaining PFHF on ITO working electrode were as follows: potential range 0.00 V- 1.30 V, voltage scan rate 100 mV/s and monomer concentration 1.4×10^{-2} M.

2.3. Characterization of Polymers

2.3.1. Cyclic Voltammetry (CV)

Cyclic Voltammetry (CV) is the most preferable electroanalytical technique due to its well-rounded and simple use. In this study, all the measurements were done at room temperature. There must be three electrodes; working electrode (WE), counter electrode (CE) and finally reference electrode (RE) in a properly working system. In CV, potentiostat linearly scans the potential on WE with previously defined scan rate in a triangular waveform (Figure 19). Figure 20 shows the monitored voltogram for a reversible reaction just after a single potential cycle. As the potential is applied to the system, current is created from WE to CE and potentiostat detects that current flow.

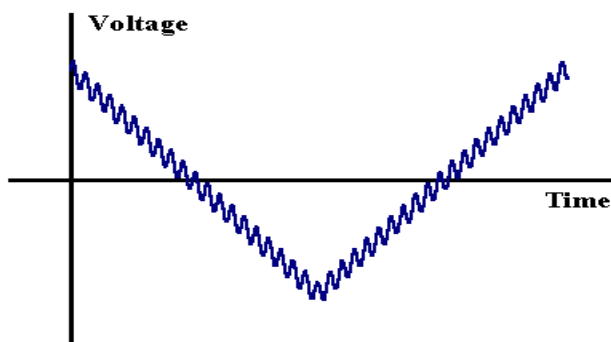


Figure 19. CV waveform.

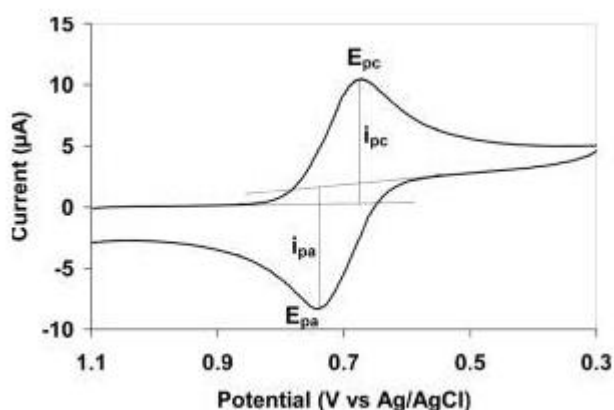


Figure 20. CV for a reversible anodic oxidation and reduction process.

Randles-Sevcik equation defines a relation between peak heights (i_p) and concentration of the monomer.

$$i_p = 0.4463nFAC(nFvF/RT)^{1/2} \quad \text{or} \quad i_p = (2.687 \times 10^5) n^{3/2} v^{1/2} D^{1/2} A C$$

n: the number of the electrons

F: Faraday Constant (96485 C/mol)

A: Area of the electrode (cm^2)

C: Concentration

V: Scan rate (V/sec)

R: Universal Gas Constant (8.314 J/molK)

T: Temperature (K)

D: Diffusion Coefficient (cm^2/sec)

As the equation implies, peak current height is directly proportional to the concentration while it is proportional to square root of scan rate. However; in the equation, there is diffusion coefficient factor (D) showing that redox should be diffusion controlled to obey the equation.

However; in electrochemical polymerization, polymer is coated on WE. Since polymer is deposited on the surface of the electrode, redox process is not diffusion controlled and Sevcik equation is not valid any more.

2.4. Spectroelectrochemistry

As the name implies spectroelectrochemistry (SPEL) is the combination of spectroscopic and electroanalytic methods and provides information both on the changes in electronic transitions of CPs during the redox switching and also about the E_g values of the conjugated polymer.

- SPEL measurements were carried out with a Hewlett-Packard 8453A diode array UV-VIS spectrometer utilizing a well-considered designed three-electrode cell to allow potential application as monitoring the absorption spectra. An ITO electrode was used as a WE (Delta Tech. 8-12 Ω , 0.7 cm x 5 cm). A Pt wire and a Ag wire were used as CE and pseudo-reference electrode, respectively. All electrodes were connected to a potentiostat.

2.5. Kinetic Properties

CPs should have the ability to switch rapidly between T_{colored} and T_{bleached} stages by showing colors that are observed by naked eye to be applicable as electrochromic materials. Actually, absorbance bands that have been obtained during SPEL analysis give ideas about these colors. To observe optical properties such as coloration efficiency (CE), switching time (t_s) and electrochromic contrast (highest $\Delta\%T$), again three-electrode system has to be used since the analysis is the combination of optical spectroscopy and square wave potential. As in SPEL analysis, WE is ITO electrode, RE is Ag wire and CE is Pt wire.

CHAPTER 3

RESULTS AND DISCUSSION

3.1. Electrochemical Properties of Monomers

3.1.1. Cyclic Voltammograms of Monomers

CV was used to determine the electrochemical behavior of monomers FOF, FFF, FHF and the smaller units that form the monomers furan, fluorene, fluorenone and 9,9-dihexylfluorene. 0.1 M TBAH/DCM solution was preferred for investigating the electrochemical properties of all monomers since the solubility of the materials in DCM is quite sufficient. The voltammogram of FOF exhibited an irreversible peak at 1.36 V vs. Ag/AgCl during the anodic scan. In the case of FFF and FHF, the irreversible oxidation peaks appeared at 1.08 and 1.26 V vs. Ag/AgCl in the same solvent-electrolyte couple, respectively (Figure 21). These irreversible oxidations correspond to the transfer of an electron from HOMO of the monomer molecule to the working electrode of the electrochemical system. An inspection of Figure 22 reveals that, among the three monomers, synthesized in this study, FOF has the highest oxidation potential. This is expected since FOF bears an electron withdrawing carbonyl group. This group lowers the electron density in the molecule and makes its oxidation relatively difficult.

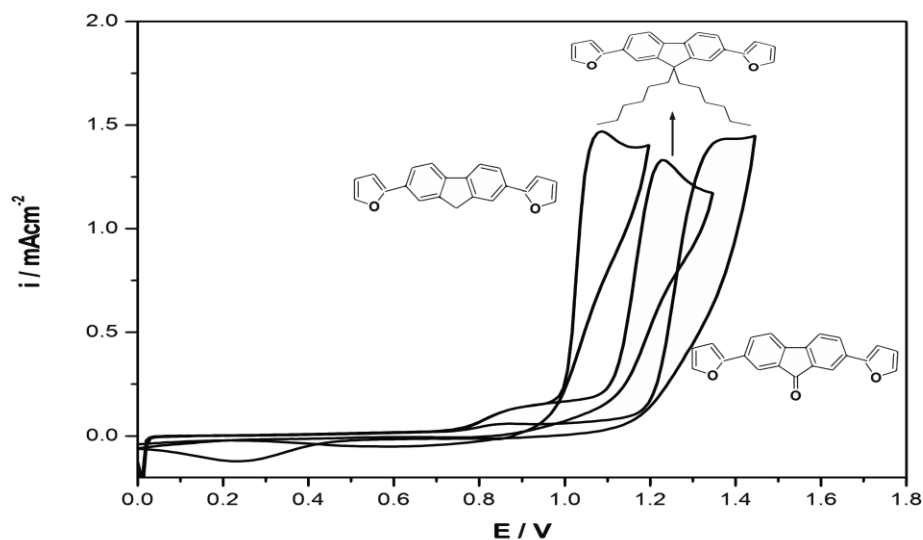


Figure 21. Cyclic voltammograms of FOF, FFF and FHF in 0.1 M TBAH/DCM solution at 100 mV/s vs. Ag/AgCl. Concentration of monomers: FOF= 4.0×10^{-3} M, FFF= 6.0×10^{-3} M, FHF= 8.0×10^{-3} M.

For comparison sake, cyclic voltammograms of furan and fluorene units of the monomers, FOF, FFF and FHF were also recorded in 0.1 M TBAH/ACN medium and results are shown in Figure 22. As it is seen from Figure 22, the oxidation potentials of three monomers synthesized in this work are smaller than that of their smaller heterocyclic units ($E_{ox} = 1.72$ V for furan, $E_{ox} = 1.82$ V for fluorene, $E_{ox} = 1.87$ V for 9,9-dihexylfluorene and $E_{ox} = 2.15$ V for fluorenone). This shift can be explained on the basis of increasing π -electron conjugation along the monomer molecules, which makes the loss of electron easier.

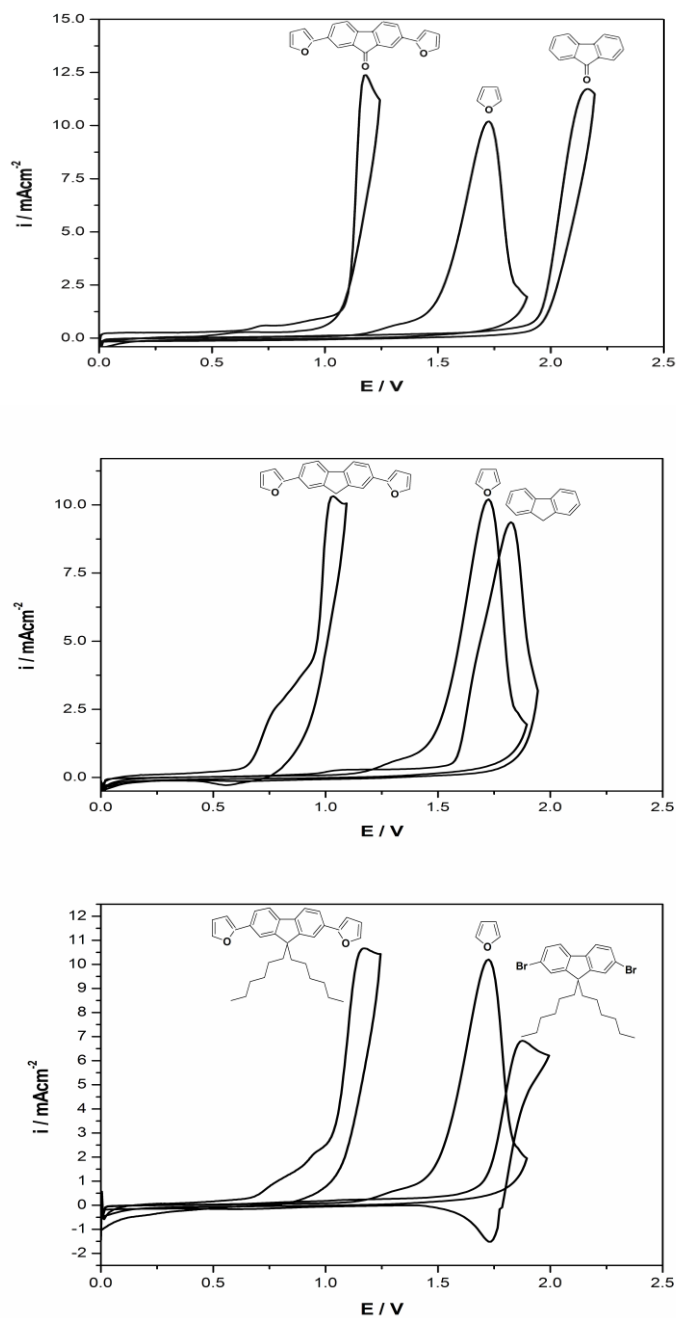


Figure 22. Cyclic voltammograms of (a) FOF, furan and fluorenone. (b) FFF, furan and fluorene (c) FHF, furan and 2,7-dibromo-(9,9) dihexylfluorene, respectively. In 0.1 M TBAH/ACN solution at 100 mV/s vs. Ag/AgCl. Concentration of monomers: Furan= 2.0×10^{-3} M, Fluorenone= 6.0×10^{-3} M, FOF= 4.0×10^{-3} M, Fluorene= 2.0×10^{-3} M, FFF= 4.0×10^{-3} M, 2,7-dibromo-(9,9)dihexylfluorene= 16.0×10^{-3} M, FHF= 8.0×10^{-3} M.

3.1.2. Electropolymerization of Monomers

Electropolymerization of the monomers was achieved via repetitive cycling in 0.1 M TBAH solutions. Due to solubility limitations, different solvents or solvent mixtures were used for the polymer synthesis. Since solubility of FOF in ACN was limited, it was first dissolved in DCM and the resulting solution was added to ACN containing 0.1 M TBAH (3/97, v/v). In the case of FFF, DCM was used as the solvent. Since the polymer formed during repetitive cycling of FHF solution was soluble in DCM, ACN was preferred as solvent for the electrochemical polymerization of FHF. In the case of FOF and FFF, it was possible to obtain deposition of polymer films on the surface of Pt or ITO working electrode surfaces. Although no polymer deposition was observed on the Pt working electrode surface in the case of FHF monomer, electrodeposition of PFHF was successfully achieved onto ITO electrode. Thus, only ITO working electrode was used for the synthesis and characterization of PFHF. During potential cycling of electrolyte solutions containing the corresponding monomers, new reversible redox couples appeared at about 1.08 V for FOF, 0.92 V for FFF and 0.96 V for FHF during repetitive anodic scans (Figure 23). These new reversible redox couples gain intensity during the repetitive anodic scans indicating the formation of electroactive polymer films on the surface of working electrode with increasing polymer film thickness.

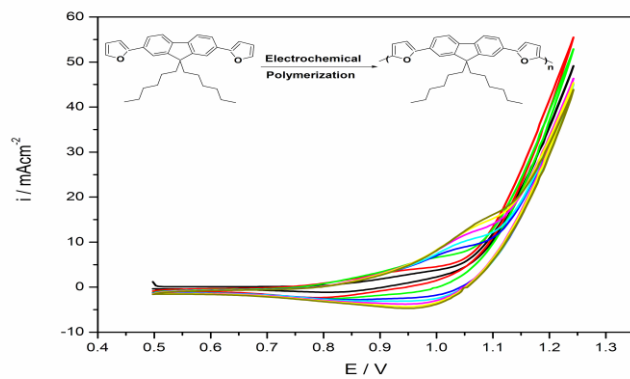
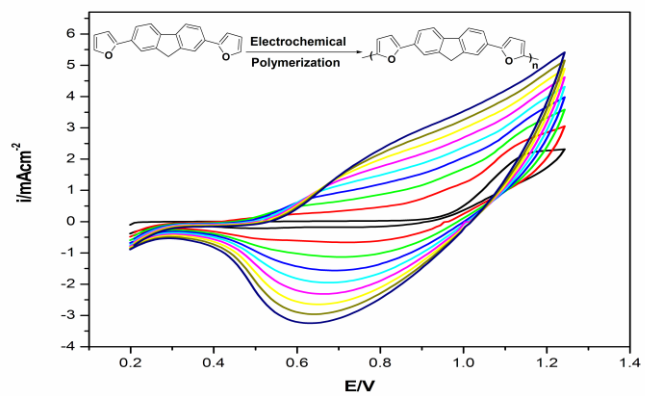
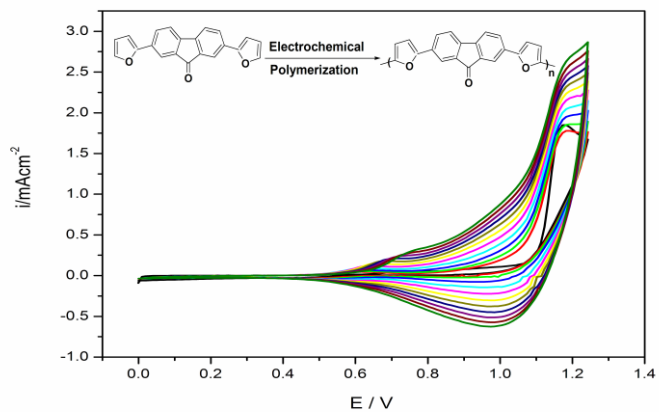


Figure 23. Electropolymerization of 4.0×10^{-3} M of FOF in DCM/ACN (3/97;v/v), 6.0×10^{-3} M of FFF in DCM and 14.0×10^{-3} M of FHF in ACN with 0.1 M TBAH at 100 mV/s (vs. Ag/AgCl).

3.2. Characterization of Polymers

3.2.1. FTIR Spectroscopy

For the quantitative analysis of the polymers, the polymer films were synthesized via constant potential electrolysis at 1.25 V vs Ag/AgCl. The polymer films formed after the electrolysis were washed with ACN and then dried. The FTIR spectra of polymer films, PFOF, PFFF and PFHF and their corresponding monomers were recorded and given in Figure 24. Since the monomers, FOF, FFF and FHF are prepared by combining two aromatic rings via Stille coupling. Prior to interpretation of the IR spectra of monomers, their corresponding polymers, and also their aromatic units, namely furan and fluorene moieties were recorded. In the case of furan moiety, the characteristic peaks appear at 3150 and 3128 cm^{-1} due to aromatic ring stretching, 1586 and 1487 cm^{-1} due to symmetric C=C ring stretching, 1171 cm^{-1} due to C-O-C stretching, 1050 and 985 cm^{-1} due to C-H in plane deformation, 915 and 865 cm^{-1} due to in plane and out of plane deformation of five membered aromatic ring [95]. On the other hand, the fluorene moiety exhibits the following characteristic peaks; 2850-2960 cm^{-1} due to aromatic C-H stretching, 1598 and 1453 cm^{-1} due to C=C ring stretching, 1260 cm^{-1} due to C-C inter ring stretching and the peak at 740 cm^{-1} indicates the 1,2-disubstituted benzene rings of fluorene precursor [96]. When the monomers FOF, FFF and FHF are formed after the coupling reaction the peak that appears around 740 cm^{-1} indicating the 1,2-disubstituted benzene ring disappears and a new peaks appears at around 840 cm^{-1} and 960 cm^{-1} which are characteristic of 1,2,4-trisubstituted benzene rings. Furthermore, in the FTIR spectrum of FOF the characteristic carbonyl peak at 1720 cm^{-1} and in the FTIR spectrum of FHF the characteristic aliphatic C-H stretching remained unchanged indicating that these groups remain intact upon formation of monomers. A comparison of FTIR spectra of monomers with their corresponding polymers (Figure 24 a,b and c) indicates that the most prominent change is the disappearance of the peak due to α -C-H stretching of furan ring (822 cm^{-1} peak for FFF and FHF and 840 cm^{-1} for FOF). Another noticeable feature in the spectra of polymers is the existence of a new peak at around 920 and 850 cm^{-1} , which is characteristic of disubstituted five-membered aromatic

ring, suggesting that α -position in the polymer are involved in the polymerization. In addition, the new sharp peak appearing 835 cm^{-1} indicates the presence of PF_6^- dopant anion.

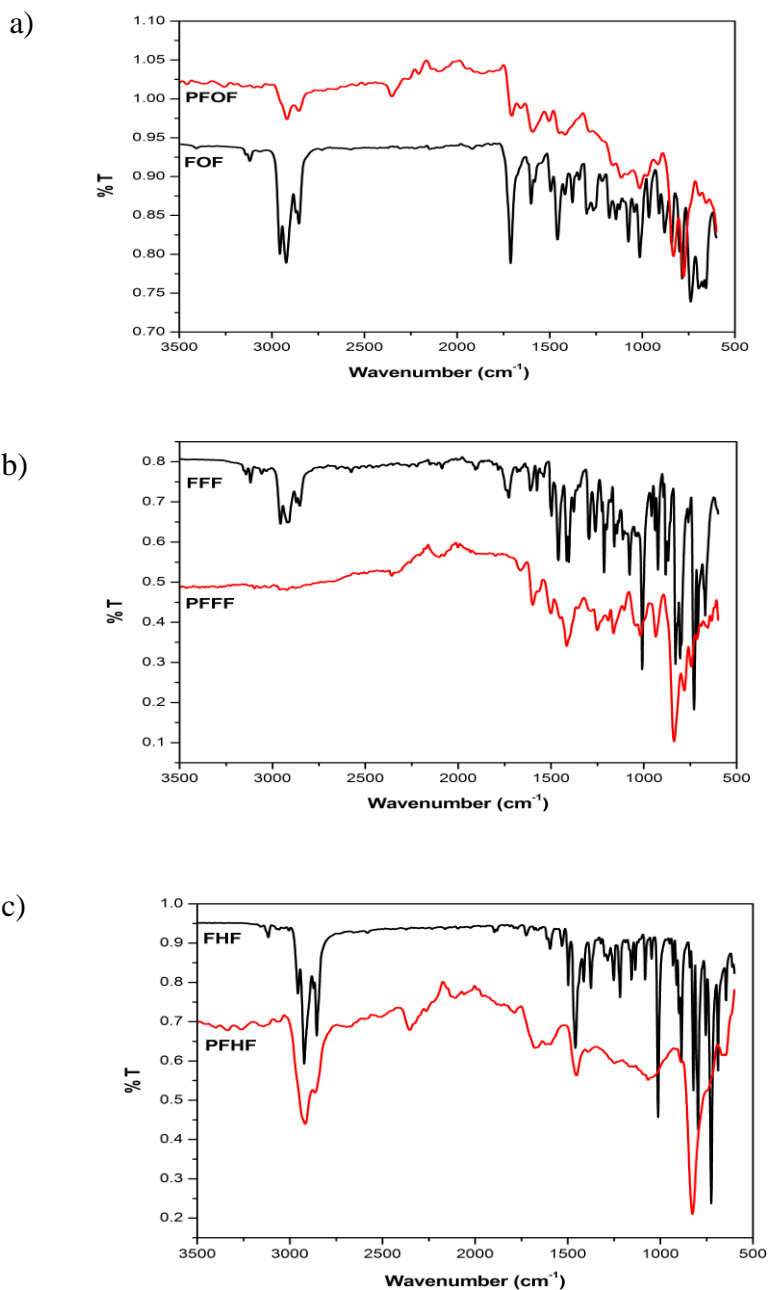


Figure 24. FTIR spectra for monomers and their polymers a) FOF, PFOF b) FFF, PFFF c) FHF,PFHF.

3.2.2. Thermal Gravimetric Analysis (TGA)

Thermal gravimetric analysis of the polymers were performed with 10°C/min heating rate under nitrogen atmosphere to characterize the thermal stability of polymers. The results are depicted in Figure 25.

In the case of PFOF, there was no evidence for decomposition of polymer until 100 °C; however, beyond this temperature, a gradual weight loss was started. PFOF was the most thermally stable polymer among the three polymers since it conserved more than 30 % of its initial weight when heated to 950 °C. PFFF decomposed 100 % until 920 °C while fully decomposition temperature for PFHF was 700 °C (Figure 25).

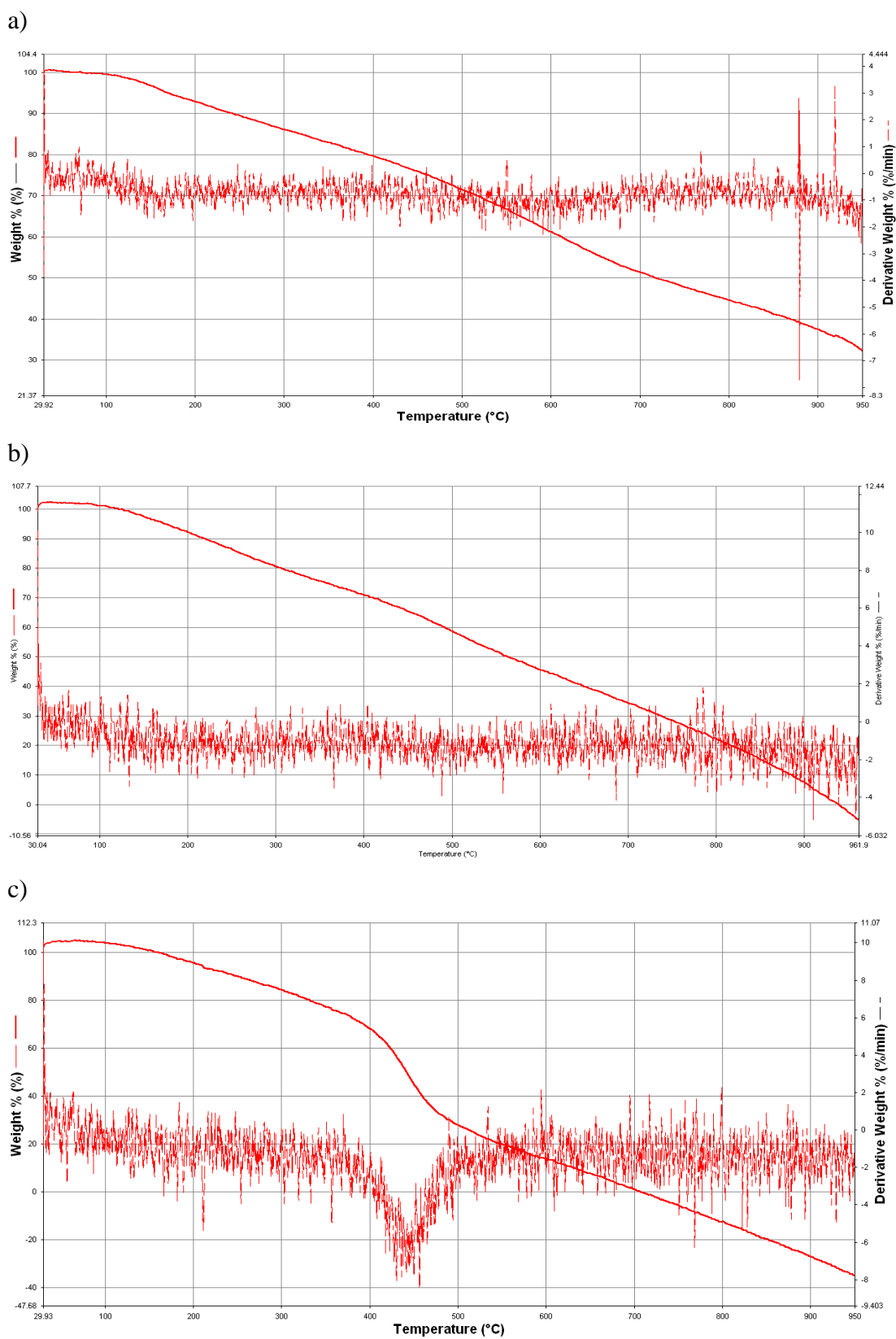


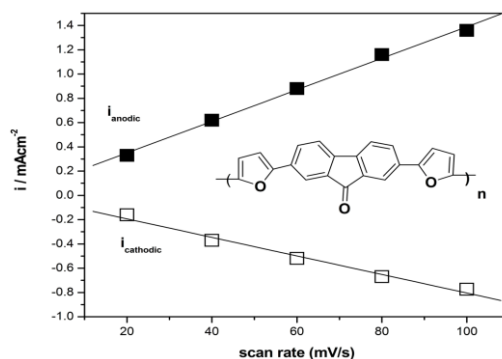
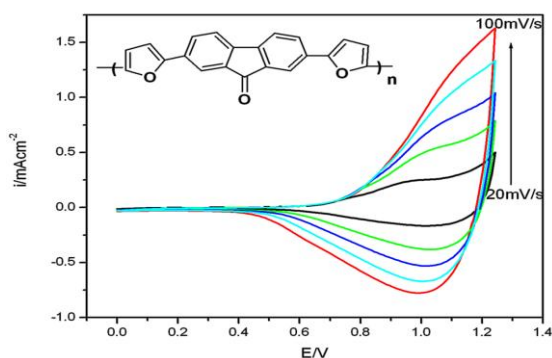
Figure 25. Thermograms for a) PFOF, b) PFFF, c) PFHF.

In addition, FTIR spectroscopy was used to characterize the gases that came out from the polymers during thermal decomposition. As in the case of all hydrocarbons, CO₂ gas and H₂O vapor were the expected products for burning reaction. CO₂ molecule has two different peaks resulting from asymmetrical stretching at 2400 cm⁻¹ and bending at 666 cm⁻¹ in its FTIR spectrum. Moreover; H₂O molecule has three different peaks that belongs to symmetric stretching, asymmetric stretching and bending at 3657 cm⁻¹, 3755.9 cm⁻¹ and 1594.7 cm⁻¹, respectively. These proper peaks at well defined frequencies were observed in the FTIR spectra of out-coming gases for all three polymers. As the time passing, the intensity of the peaks were increasing due to the increase in the amount of decomposition of polymers (Appendix B).

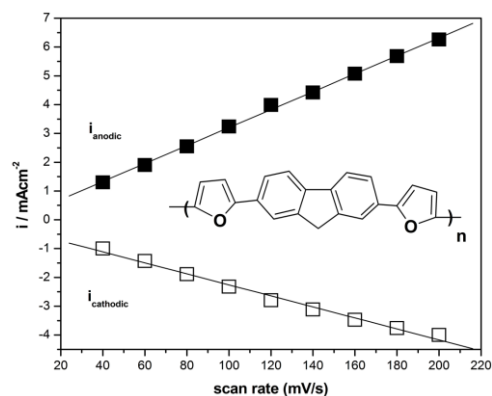
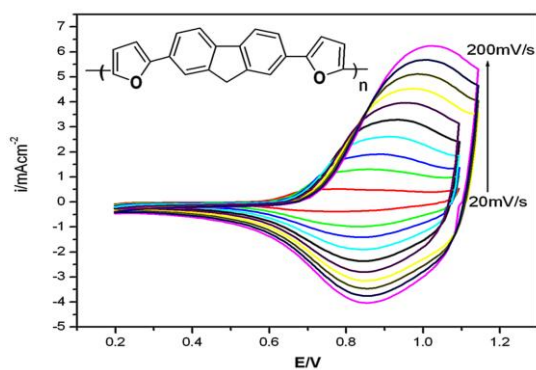
3.3. Electrochemical Properties of Polymers

Electrochemical behaviors of polymer films that were deposited on the working electrode surface were investigated in monomer free electrolytic solution containing 0.1 M TBAH/ACN and resulting voltammograms are shown in Figure 26. As it seen from the figure PFOF, PFFF and PFHF exhibited single and well-defined reversible redox couples at 1.083 V, 0.915 V and 0.985 V, respectively. A linear increase in the peak currents as a function of the scan rates confirmed well-adhered electroactive polymer films on the electrode surface as well as non-diffusional redox process.

(a)



(b)



(c)

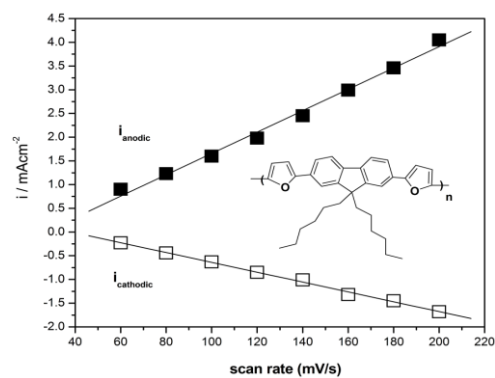
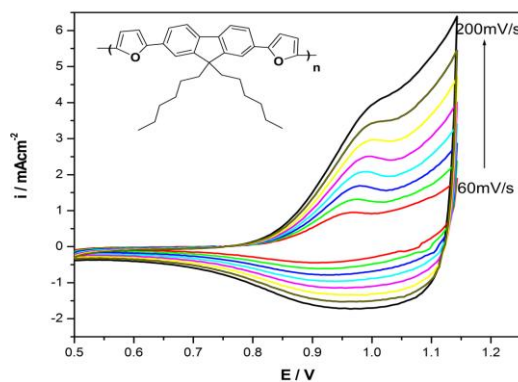


Figure 26. Scan rate dependence of polymer films on a Pt disk electrode in 0.1 M TBAH/ACN and relationship of anodic ($i_{p,a}$) and cathodic ($i_{p,c}$) current peaks as a function of scan rate between neutral and oxidized states of (a) PFOF film (b)PFFF film (c) PFHF film in 0.1 M TBAH/ACN (vs.Ag/AgCl).

3.4. Stability of Polymer Films

The electrochemical stability of the material upon switching or cycling is one of the important parameters for technological applications. There are two common methods to test the electrochemical stability of materials; i) potential scanning between neutral and oxidized states and ii) cycling. In this study, the stability of PFOF, PFFF and PFHF films were investigated by cycling method under nitrogen atmosphere. Therefore, polymer films were coated on ITO electrode via repetitive cycling (20 repetitive cycling) and then cyclic voltammograms of polymer films were recorded in monomer free electrolytic solution in the potential range that includes fully oxidized and reduced forms of polymers. The potential range was 0.00 V to 1.15 V for PFOF while it was 0.00 V to 1.10 V for PFFF and 0.50 to 1.10 for PFHF. Cycling was done with a scan rate of 500 mV/s for all polymers and after each 200 cycles, cyclic voltammograms of the films were recorded by CV with a scan rate that is proper for the film. As shown in Figure 27, the electrochemical stabilities of polymer films were not so good; however, they still have some of their electro activity after 1000 cycles. After first 200 cycles PFOF lost 21 % of its electroactivity while PFFF and PFHF lost 13 % and 40 %, respectively. In addition, after second 200 cycles PFOF, PFFF and PFHF lost 24 %, 12 % and 23 % of the electroactivity that remained after first 200 cycles, respectively. If the polymer films compared, PFFF is the most stable one since it lost only 24 % of its initial electroactivity after 400 cycles while the lost amount was 40 % and 61 % for PFOF and PFHF, respectively. Finally, after 1000 cycles, PFOF, PFFF and PFHF lost 68 %, 52 % and 80 % of their initial electroactivity, respectively.

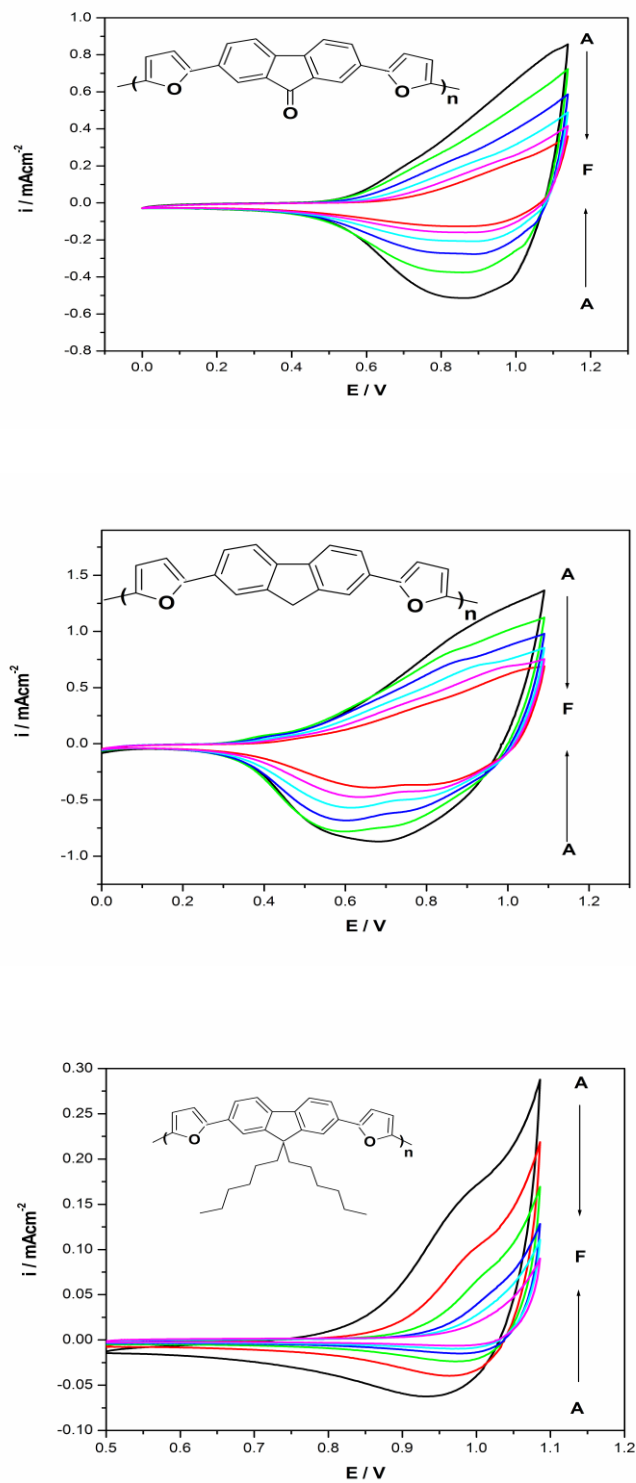


Figure 27. Stability test for PFOF, PFFF and PFHF films in 0.1 M TBAH/ACN as a scan rate of 60 mVs^{-1} , 80 mVs^{-1} , 100 mVs^{-1} respectively under nitrogen atmosphere by CV as a function of : A: 1st; B: 200th; C: 400th; D: 600th; E: 800th, F: 1000th cycles.

3.5. Spectroelectrochemical Properties of Polymers

The electro-optical properties of the polymer films, deposited on ITO working electrode via constant potential electrolysis, were investigated by monitoring the changes in the electronic absorption spectra under a voltage pulse in a monomer free electrolyte solution. The results are depicted in Figure 28. The electronic absorption spectra of neutral forms of the films exhibit an absorption band at around 350, 380 and 367 nm for PFOF, PFFF and PFHF, respectively. These bands are due to π - π^* transition and they all lose intensity during oxidation which is accompanied by the appearance of new intensifying bands.

In the case of PFOF, as the valance-conduction band at 350 nm diminishes a new band starts to intensify at about 690 nm in the potential range of 0.0 to 0.90 V. Upon further oxidation, beyond 0.90 V, this band undergoes a blue shift to 620 nm, which is accompanied with the formation of a weak broad band around 940 nm. Appearance of these new bands indicates the formation of charge carriers. All spectra recorded during potential cycling between 0.0 and 1.20 V passes through a clear isosbestic points at 440 nm, indicating that polymer film was being interconverted between its neutral and oxidized states. The changes in the electronic absorption spectra of PFOF film are also accompanied by a color change, orange to green, indicating that PFOF film exhibits electrochromic behavior. In the case of PFFF, the new band due to the formation of charge carriers appears at about 650 nm and is accompanied with an electrochromic response from yellow to dark blue. The SPEL changes recorded for PFHF film, on the other hand, are different than those of PFOF and PFFF in terms of the formation of two absorption bands at about 660 and 780 nm, indicating the formation of charge carriers, polarons and bipolarons, respectively. PFHF film also exhibits electrochromic response and its color changes from orange to green as the polymer film is transformed from neutral to oxidized state. The electrochromic response of all three polymer films are given in Table 1.

The band gap values of polymer films deposited on ITO electrodes via constant potential electrolysis were also determined from the commencement of low energy

end of π - π^* transitions (i.e., 350, 380 and 367 nm for PFOF, PFFF and PFHF, respectively), and the following values were found 2.32, 2.49 eV and 2.61 eV for PFOF, PFFF and PFHF, respectively.

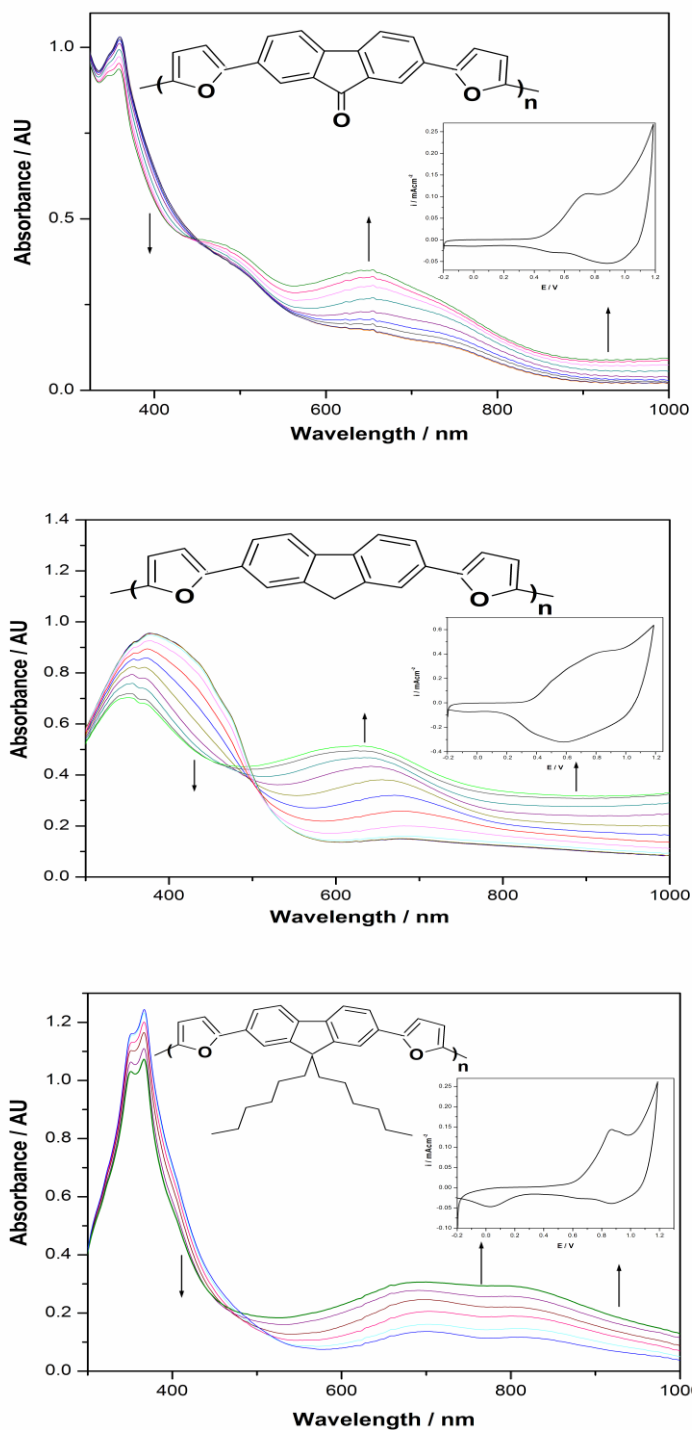








Figure 28. Optical absorption spectra of PFOF, PFFF and PFHF on ITO electrode in 0.1 M TBAH/DCM at potential range between -0.20 and 1.20 V. Inset Cyclic voltammograms recorded during potential scanning in monomer free solution.

Table 1. Colors of the PFOF, PFFF and PFHF, on ITO electrodes in their neutral and oxidized state.

	PFOF	PFFF	PFHF
Neutral State			
Oxidized State			

3.6. Kinetic Properties of Polymers

Due to its importance in electrochromic applications, switching times and optical contrast of the polymer films on ITO were also investigated under square wave input of 0.0 V to 1.2 V in 10 s intervals by monitoring the visible transmittance. The kinetic responses of the film at various wavelengths are depicted in Figure 29. The percentage transmittance change ($\Delta\%T$) between the neutral (at 0.0 V) and oxidized states (at 1.20 V) of PFOF film was found to be 14.2 % for 655 nm. While it was 13.5 % for PFFF at 615 nm and it was 6.7 % for PFHF at 721 nm between neutral and oxidized states (Figure 29).

The CE was found to be 20.25 cm²/C at 638 nm (a response time 1.54 s) for PFOF film, 101.6 cm²/C at 615 nm (a response time 2.58 s) for PFFF film and 95.94 cm²/C at 534 nm (a response time 1.55 s) PFHF film. Although percentage transmittance values for all three polymers were found to be low, the CE values for PFOF and PFHF seems to be reasonable when compared to other polyfluorene derivatives. To illustrate, when furan units in PFOF was changed with thiophene units, CE value was founded to be 46.80 cm²/C at 697 nm [54].

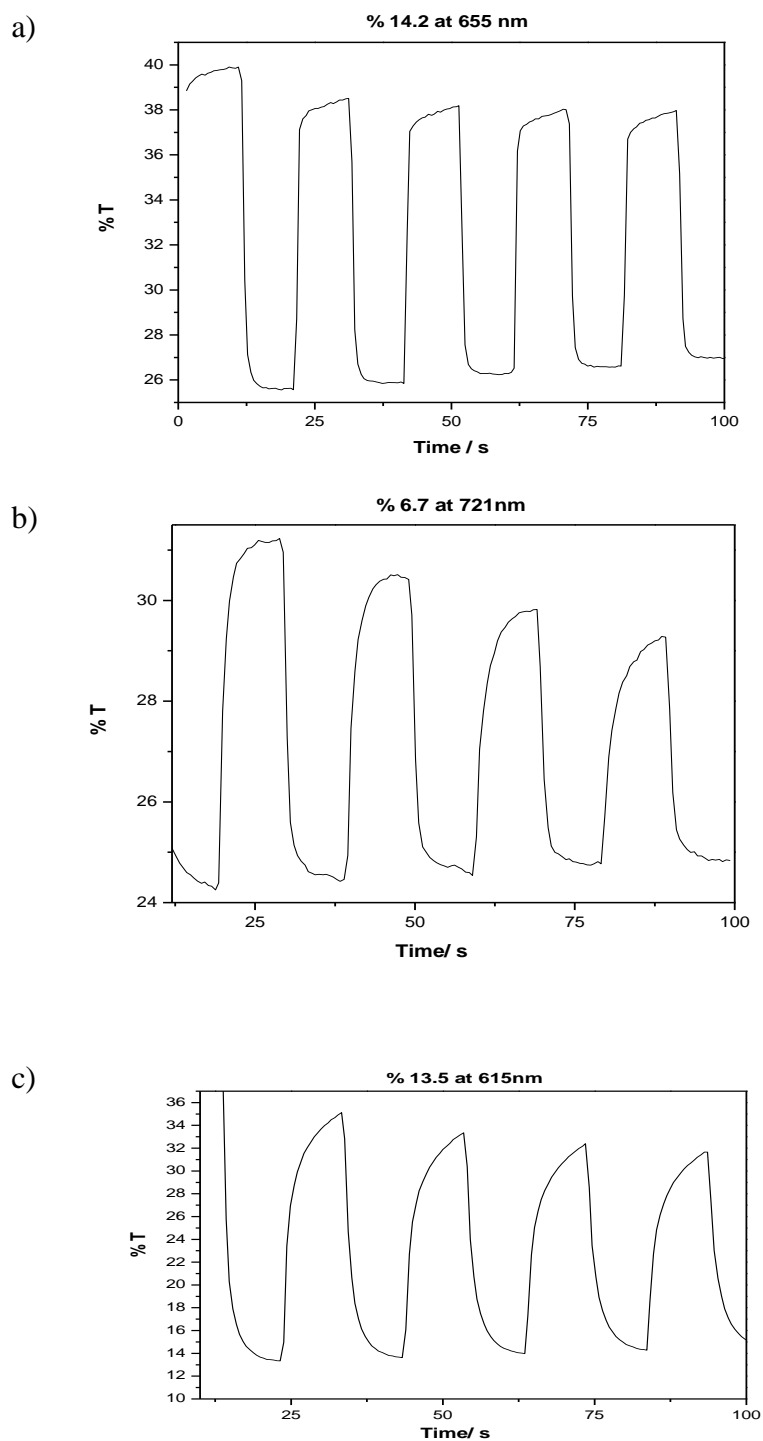


Figure 29. Chronoabsortometry experiments for (a) PFOF film switched between 0.0 V and 1.15 V (b) PFFF film switched between 0.0 V and 1.20 V. (c) PFHF film switched between 0.0 V and 1.20 V with an interval time of 10 s on ITO in 0.1 M TBAH/ACN vs. Ag wire.

Table 2. Optical and electrochemical properties of PFOF, PFFF and PFHF.

	PFOF	PFFF	PFHF
E_m^{ox} (V)	1.36	1.08	1.26
λ_{max} (nm)	350	380	367
E_g (eV)	2.32	2.49	2.61
$\Delta\%T$	14.2	13.5	6.7
Color	Orange (neut.) Green (ox)	Yellow (neut.) Dark Blue (ox)	Orange (neut.) Green (ox)
t_s (s)	1.55	2.58	2.66
ΔOD	0.022	0.09	0.0434
$Q_{d95\%}$ (mC/cm ²)	1.1×10^{-3} (638 nm)	8.9×10^{-4} (615 nm)	5.1×10^{-4} (721 nm)
$CE_{95\%}$ (cm ² /C)	20.25	101.6	84.58
HOMO	-5.205	-5.089	-5.229
LUMO	-2.885	-2.599	-2.619

3.7. Chemical Polymerization of FHF

Yamamoto coupling has been frequently used for the polymerization of aryl halides to synthesize light emitting CPs such as, poly(9,9-dihexylfluorene) [46], one of the monomers (FHF), synthesized in this thesis, was also tried to be polymerized by using this method. In Yamamoto method, it is necessary for the monomer to have halide groups. Therefore, as a first step FHF was brominated using N-bromosuccinimide (NBS)(Figure 30). The reason for using NBS in bromination process is the difficulty in handling elemental bromine. It was previously reported that the addition of NBS to DMF is not very exothermic [98] so DMF was chosen to be the solvent for the reaction to control the reaction temperature. In brominating FHF, 2 equiv. NBS in DMF was added dropwise to the reaction medium that contains FHF (1 equiv.) also dissolved in DMF for an hour at room temperature. The reaction was allowed to proceed overnight and its work up was done by brine solution-DCM extraction. For the Yamamoto coupling polymerization of FHFBr (Figure 31), Ni(COD)₂ (1 equiv.), bipyridine (1 equiv.) and 1,5-cyclooctadiene (1

equiv.) were dissolved in 4 mL DMF and then refluxed for 30 minutes at 85 °C. FHFBr was dissolved in 1 mL DMF and injected to the reaction mixture. Polymerization reaction was allowed to proceed for 5 days. In standard Yamamoto coupling procedure, product is purified by HCl extraction, however, in PFHF case, this procedure can not be used since it will open the furan ring.

Brine solution-chloroform extraction was used to purify the polymer. After the extraction the organic phase was evaporated and re-dissolved in slightly acidified ethyl alcohol. Soluble and insoluble part was separated from each other by centrifuging. The solid was dried in vacuum oven and used for the characterization of the product. The soluble part was isolated by evaporating the solvent, ethyl alcohol, dried and used for the characterization.

Resulting polymer was characterized via FTIR spectroscopy (Appendix C). When the FTIR spectra of PFHF that was obtained by electrochemical and chemical polymerizations were compared, it was observed that they have the same principle peaks at almost 2921 cm^{-1} , 2854 cm^{-1} , 1670 cm^{-1} , 1604 cm^{-1} and 821 cm^{-1} . Moreover, FTIR spectrum of FHF and chemically synthesized PFHF were compared to observe disappearance of C-H stretching resulting from α -H of furan ring. In the FTIR spectrum of FHF there is a peak at 3117 cm^{-1} for α -C-H stretching while it is not present in the spectrum of PFHF. On the other hand, there is a peak at 722.83 cm^{-1} in monomer spectrum that is disappearing in the polymer spectrum with the formation of a new peak at 771.12 cm^{-1} .

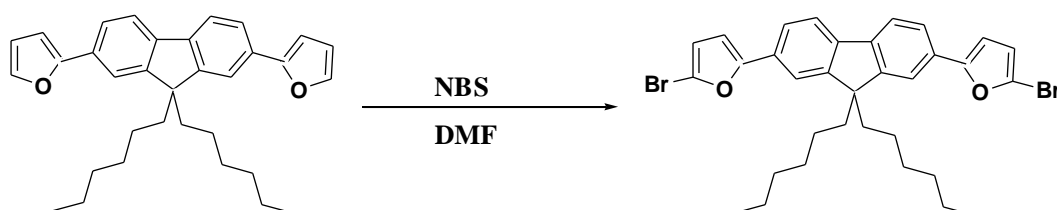


Figure 30. Bromination of FHF.

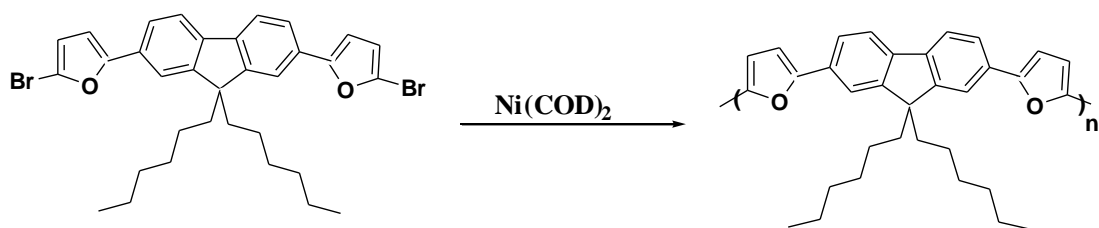


Figure 31. Chemical polymerization of FHF via Yamamoto coupling.

CHAPTER 4

CONCLUSIONS

Furan-fluorene units containing a novel series of monomers 2,7-di(furan-2-yl)-9H-fluoren-9-one (FOF), 2-(2-(furan-2-yl)-9H-fluoren-7-yl)furan (FFF), and 2-(2-(furan-2-yl)-9,9-dihexyl-9H-fluoren-7-yl)furan (FHF) were synthesized and they were characterized by spectroscopic techniques (^1H NMR, ^{13}C NMR and FTIR). In addition, polymers of the monomers PFOF, PFFF and PFHF, were synthesized by electrochemical methods such as potential cycling and constant potential electrolysis. Characterization of polymers was performed by cyclic voltammetry, FTIR spectroscopy and TGA.

TGA results revealed that PFOF was the most thermally stable polymer among the three polymers and retains more than 30 % of its initial weight at about 950 °C. Polymer films, PFOF, PFFF and PFHF, deposited on ITO electrode via potential cycling showed reversible redox behavior accompanied with a reversible electrochromic behavior; orange to green for PFOF, yellow to dark blue for PFFF and orange to green for PFHF.

Chronoabsorptometry experiments revealed that the percentage transmittance values for all three polymers were found to be low. On the other hand, the polymers have reasonably high CE .

In addition, the band gap values (E_g) of polymers were found to be 2.32, 2.49 and 2.61 eV for PFOF, PFFF and PFHF, respectively.

REFERENCES

1. C. K. Chiang, C. R. Fincher, Y. W. Park, A. J. Heeger, H. Shirakawa, E. J. Louis, S. C. Gau, and A. G. MacDiarmid, *Phys. Rev. Lett.*, 1977, 39 (17):1098.
2. H. Shirakawa, E. J. Louis, A. G. MacDiarmid, C. K. Chiang, and A. J. Heeger, *J. Chem. Soc. Chem. Commun.*, 1977, 16:578.
3. (a) H. Shirakawa, *Angew. Chem. Int. Ed.*, 2001, 40 (14):2575; (b) H. Shirakawa, *Synth. Met.*, 2002, 125 (1):3.
4. (a) A. MacDiarmid, *Angew. Chem. Int. Ed.*, 2001, 40 (14):2581; (b) A. MacDiarmid, *Synth. Met.*, 2002, 125 (1):11.
5. (a) A. J. Heeger, *Angew. Chem. Int. Ed.*, 2001, 40 (14):2591; (b) A. J. Heeger, *Synth. Met.*, 2002, 125 (1): 23.
6. A. Watanabe, S. Murakami, K. Mori, and Y. Kashiwaba, *Macromolecules*, 1989, (22): 4231.
7. M. Leclerc, and K. Farid, *Adv. Mater.*, 1997, 9, 1087.
8. R. D. McCullough, *Adv. Mater.*, 1998, 10, 93.
9. M. Leclerc, *Adv. Mater.*, 1999, 11, 1491.
10. M. Fukuda, K. Sawaka, and K. Yoshino, *J. Polym. Sci. A*, 1993, 31, 2465.
11. G. D'Aprano, M. Leclerc, and G. Zotti, *Macromolecules*, 1992, 25, 2145.
12. A. G. MacDiarmid, and A. J. Epstein, *Synth. Met.*, 1994, 65, 103.
13. J. F. Morin, and M. Leclerc, *Macromolecules*, 2001, 34, 4680.
14. J. H. Burroughes, D. D. C. Bradley, A. R. Brown, R. N. Marks, H. Friend, P. L. Burns, and A. B. Holmes, *Nature*, 1990, 347, 539.

15. (a) P. K. H. Ho, D. S. Thomas, R. H. Friend, and N. Tessler, *Science* 1999, 285, 233.; (b) I. Schwendeman, R. Hickman, G. Sonmez, P. Schottland, K. Zong, D.M. Welsh, and J.R. Reynolds, *Chem. Mater.*, 2002, 14, 3118.
16. N. S. Sariciftci, L. Smilowitz, A. J. Heeger, and F. Wudl, *Science* 1992, 258 1474.
17. H. Koezuka, and A. Tsumura, *Synth. Met.*, 1989, 28, C753.
18. j. Miasik, A. Hooper, and B. C. Tofield, *J. Chem. Soc. Farad. Trans. Phys. Chem. in Cond. Pha.*, 1986, 82, 1117.
19. R. G. Mortimer, *Chem. Soc. Rev.*, 1997, 26, 147.
20. J. Roncali, *Chem. Rev.*, 1992, 92, 711.
21. G. Zotti, *Handbook of Organic Conductive Molecules and Polymers*, ed. H. S. Nalwa, Wiley, Chichester, 1997, Vol. 2, Ch. 4.
22. G. Zotti, *Handbook of Organic Conductive Molecules and Polymers*, ed. H. S. Nalwa, Wiley, Chichester, 1997, Vol. 2, Ch. 4.
23. J. R. Reynolds, S. G. Hsu, and H. J. Arnott, *J. Polym. Sci Part B Polym. Phys.*, 1989, 27, 2081.
24. G., Zotti, R., Gumbs, *Handbook of Organic Conductive Molecules and Polymers*, ed. H.S. Nalwa, Editor. 1997, Wiley, Chichester.
25. (a) S. Asavapiriyonont, G. K. Chandler, G. A. Pletcher, and D. Gunawardena, *J. Electroanal. Chem.*, 1984, 177, 229. (b) T. Inoue, and T. Ymase, *Bull. Chem. Soc. Jpn.*, 1983, 56, 985.
26. E. Genius, G. Bidan, and A. F. Diaz, *J. Electroanal. Chem.*, 1983, 149, 113.
27. C. L. Gaupp, PhD thesis, University of Florida, 2002.
28. T. Okada, T. Ogata, and M. Ueda, *Macromolecules*, 1996, 29, 7645.
29. N. Toshima, and S. Hara, *Prog. Polym. Sci.*, 1995, 20, 155.
30. K. Yoshino, R. Hayashi, and R. Sugimoto, *Jpn. J. Appl. Phys.*, 1984, 23, 899.

31. Delabouglise, R. Garreau, M. Lemaire, and J. Roncali, *New J. Chem.*, 1988, 12, 155.
32. R. H. Baughman, J. L. Bredas, R. R. Chance, R. L. Elsenbaumer, and L. W. Shacklette, *Chem. Rev.*, 1982, 82, 209.
33. (a) J. R. Reynolds, J. P. Ruiz, A. D. Child, K. Navak, and D. S. Marynick, *Macromolecules*, 1991, 24, 678. (b) J. R. Reynolds, A. D. Child, J. P. Ruiz, S. Y. Hong, and D.S. Marynick., *Macromolecules*, 1993, 26, 2095.
34. M. Pomerantz, *Handbook of Conducting Polymers*; 2nd ed. T. A. Skotheim, R. L. Elsenbaumer, J. R. Reynolds, Ed: Marcel Dekker: New York , 1998, 227.
35. I. Schwendeman, PhD Thesis, University of Florida, 2002.
36. U. Salzner, J. B. Lagowski, P. G. Pickup, and R. A. Poirier, *Synth. Met.*, 1998, 96, 177-189.
37. J. Tanguay, M. Slama, M. Hoalet, and j. L. Baudouin, *Synth. Met.*, 1989, 28, 145.
38. P. J. Nigrey, A. G. MacDiarmid, and A. J. Heeger, *Chem. Commun.*, 1979, 96 594.
39. P. J. Nigrey, A. G. MacDiarmid, and A. J. Heeger, *J. Chem. Soc.-Chem. Commun.*, 1979, 594.
40. K. Gurunathan, A. V. Murugan, R. Marimuthu, U. P. Mulik, and D. P. Amalnerkar, *Mater. Chem. Phys.*, 1999, 61, 173.
41. P. J. Nigrey, A. G. MacDiarmid, and A. J. Heeger, *J. Chem. Soc.-Chem. Commun.*, 1979, 594.
42. D. Sainova, T. Miteva, H. G. Nothofer, U. Scherf, I. Glowacki, H. Fujikawa, and D. Neher, *Appl. Phys. Lett.*, 2000, 76, 1810.
43. A. W. Grice, D. D. C. Bradley, M. T. Bernius, M. Inbasekaran, W. W. Wu, and E. P. Woo, *Appl. Phys. Lett.*, 1998, 73, 629.

44. B. Liu, Z.-K. Chen, W.-L. Yu, Y.-H. Lai, and W. Huang, *Thin Solid Films*, 2000, 363, 332.
45. B. Liu, W.-L. Yu, Y.-H. Lai, and W. Huang, *Macromolecules* 2002, 35, 4975.
46. N. Fomina, PhD thesis, University of Southern California, 2009.
47. N. Fomina, PhD thesis, University of Southern California, 2009.
48. M. Fukuda, K. Sawada, and K. Yoshino, *Jpn. J. Appl. Phys., Part 1* 1989, 28, 1433-1435.
49. M. Fukuda, K. Sawada, and K. Yoshino, *J. Polym. Sci., Part A: Polym. Chem.*, 1993, 31, 2465-2472.
50. Y. Maleku, Msc thesis, Addis Ababa University, 2007, 36.
51. Y. Maleku, Msc thesis, Addis Ababa University, 2007, 30.
52. Y. Zekarias, MSc Thesis, Addis Ababa University, Addis Ababa, Ethiopia, 2004.
53. T. Yohannes, F. Zhang, M. Svensson, J.C. Hummelen, M.R. Andersson, and O. Inganäs, *Thin Solid Films*, 2004, 449, 152.
54. A. Kivrak, B. Carbas, and A. M. Onal, submitted to *Electrochimica Acta*.
55. G. Tournillon, and F. Garnier, *J. Electroanal. Chem.*, 1982, 135, 73.
56. T. Ohsawa, K. Kaneto, and K. Yoshino, *Jpn J Appl Phys*, 1984, 23, L663.
57. S. Glenis, M. Benz, E. LeGoff, J. L. Schindler, C. R. Kannewurf, and M. G. Kanatzidis, *J. Am. Chem. Soc.*, 1993, 115, 12519.
58. B. Nessakh., and Z.; F. Kotkowska-Machnik, *J. Electroanal. Chem.*, 1990, 296, 263.
59. G. Zotti, G. Schiavon, and N. Comisso, *Synth. Met.*, 1990, 36, 337.

60. L. Carillo, E. Sanchez de la Blanca, M. J. Gonzales-Tejera, and I. Hernandez-Fuentes, *Chem. Phys. Lett.*, 1994, 229, 633.
61. B. Demirboğa, A. M. Önal, *Synth. Met.*, 1999, 99,237.
62. X. Wan, F. Yan, S. Jin, X. Liu, and G. Xue, *Chem. Mater.*, 1999, 11, 2400.
63. S. Tirkes, and A. M. Önal, *J. Appl. Polymer Sci.*, 2007, 103, 871-876.
64. M. J. Gonz'alez-Tejera, I. Carrillo, and I. Hern'andez-Fuentes, *Synth. Met.*, 1998, 92, 187.
65. M. Kabasakaloğlu, M. Talu, F. Yildirim, and B. Sari, *Appl. Surf. Sci.*, 2003, 218, 84.
66. T. Ogawa, T. Igarashi, T. Kawanishi, T. Kitamura, and K. Hoshino, *J. Photopolym. Sci. Technol.*, 2004, 17, 143.
67. X. Wan, W. Zhang, S. Jin, G. Xue, Q.-D. You, and B. Che, *J. Electroanal. Chem.*, 1999, 470, 23.
68. L. Li, X. Wan, and G. Xue, *Chin. J. Polym. Sci.*, 2002, 20, 419.
69. M. J. Gonz'alez-Tejera, I. Carrillo, and I. Hern'andez-Fuentes, *Anal. Quim.*, 1993, 89, 4, 521.
70. M. J. Gonz'alez-Tejera, I. Carrillo, and I. Hern'andez-Fuentes, *Synth. Met.*, 1998, 92, 187.
71. A. Diaz, F. Bargon, in: T.A. Skotheim (Ed.), *Handbook of Conducting Polymers*, vol. 1, Marcel Dekker, Inc., New York, 1986, 81–115.
72. S. Sadki, P. Schottland, N. Brolic, and G. Sabouraud, *Chem. Soc. Rev.*, 2000, 29, 283.
73. M.J. Gonz'alez-Tejera, Sanchez de la Blanca, and I. Carrillo, *Synth. Met.*, 2008, 158, 165-189.

74. B. Friedel, C.R. McNeill, and N.C. Greenham, *Chem. Mater.*, 2010, 22, 3389-3398.
75. R. Kroon, M. Lenes, J.C. Hummelen, P.W.M. Blom, and B. Boer, *Polym. Rev.*, 2008, 48, 531–582.
76. P. Herguth, X. Jiang, M.S. Liu, and A.K.Y. Jen, *Macromolecules*, 2002, 35, 6094–6100.
77. A. Cirpan, L. Ding, and F.E. Karasz, *Polymer*, 2005, 46, 811–817.
78. P.M. Beaujuge and J.R. Reynolds, *Chem. Rev.*, 2010, 110, 268–320.
79. A. Argun, P.H. Aubert, B. C. Thompson, I. Schwendeman, C. L. Gaupp, J. Hwang, N. J. Pinto, D. B. Tanner, A. G. MacDiarmid, and J. R. Reynolds, *Chem. Mater.*, 2004, 16, 4401.
80. R. D. Rauh, and S. F. Cogan, *Solid State Ionics*, 1988, 28-30, 1707.
81. K. Bange, and T. Bambke, *Adv. Mater.*, 1990, 2, 10.
82. A. Dodabalapur, L. Torsi, and H. E. Katz, *Science*, 1995, 268, 270.
83. A. Kraft, A. C. Grimsdale, and A. B. Holmes, *Angew. Chem. Intl. Ed.*, 1998, 37, 402.
84. J.P. Ferraris, M.M. Eissa, I.D. Brotherson, and D.C. Loveday, *Chem. Mater.*, 1998, 10, 3528.
85. G. Heywang, and F. Jonas, *Adv. Mater.*, 1992, 4, 116.
86. P.N. Bartlett, and R.G. Whitaker, *J. Electroanal. Chem.*, 1987, 224–37.
87. (a) Bayer AG Eur. Patent 339, 334, 1988. (b) F. Jonas, and L. Schrader, *Synth. Met.* 1991, 41-43, 831. (c) G. Heywang, and F. Jonas, *Adv. Mater.*, 1992, 4, 116.

88. D.T. McQuade, A.E. Pullen, and T.M. Swager, *Chem. Rev.*, 2000, *100*, 2537.
89. J. Pernaut, and J.R. Reynolds, *J. Phys. Chem. B*, 2000, *104*, 4080.
90. B. Sankaran, and J.R. Reynolds, *Macromolecules*, 1997, *30*, 2582.
91. S.A. Sapp, G.A. Sotzing, and J.R. Reynolds, *Chem. Mater.*, 1998, *10*, 2101.
92. P. Novak, K. Muller, K.S.V. Santhanam, and O. Hass, *Chem. Rev.*, 1997, *97* 207.
93. W. Schuhmann, *Microchim. Acta.*, 1995, *121*, 1.
94. T.F. Otero, H. Grande, *Handbook of Conducting Polymers*, 1998, 2nded.; T.A, Skotheim, R.L. Elsenbaumer, J.R.Reynolds (Eds), 1998, Marcel Dekker: New York.
95. F. Alakhras, R. Holze, *J. Solid State Electrochem*, 2008, *12*, 81–94.
96. S. Zhang et al., *Electrochimica Acta*, 2006, *51*, 5738–5745.
97. L. Valentini, F. Mengoni, L. Mattiello, and J. M. Kenny, *Nanotechnology*, 2007, *18*, 115702 (5pp).
98. M. A. Raheem, J. R. Nagireddy, R. Durham, and W. Tam, *Synthetic Communications*, 2010, (40):14, 2138 – 2146.

APPENDIX A

NUCLEAR MAGNETIC RESONANCE SPECTRA OF FOF, FFF AND FHF MONOMERS

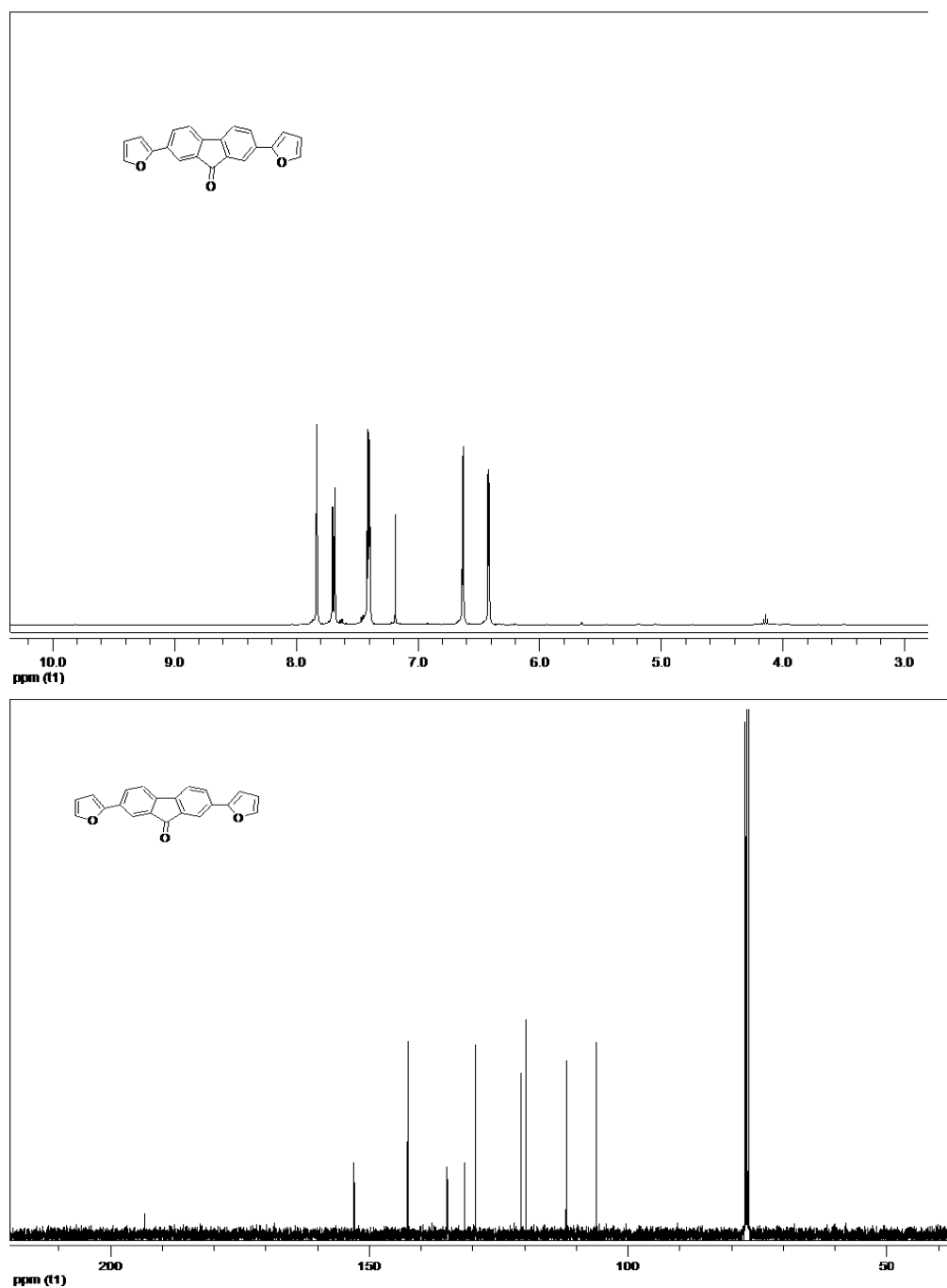


Figure A.1. ^1H NMR and ^{13}C NMR of FOF.

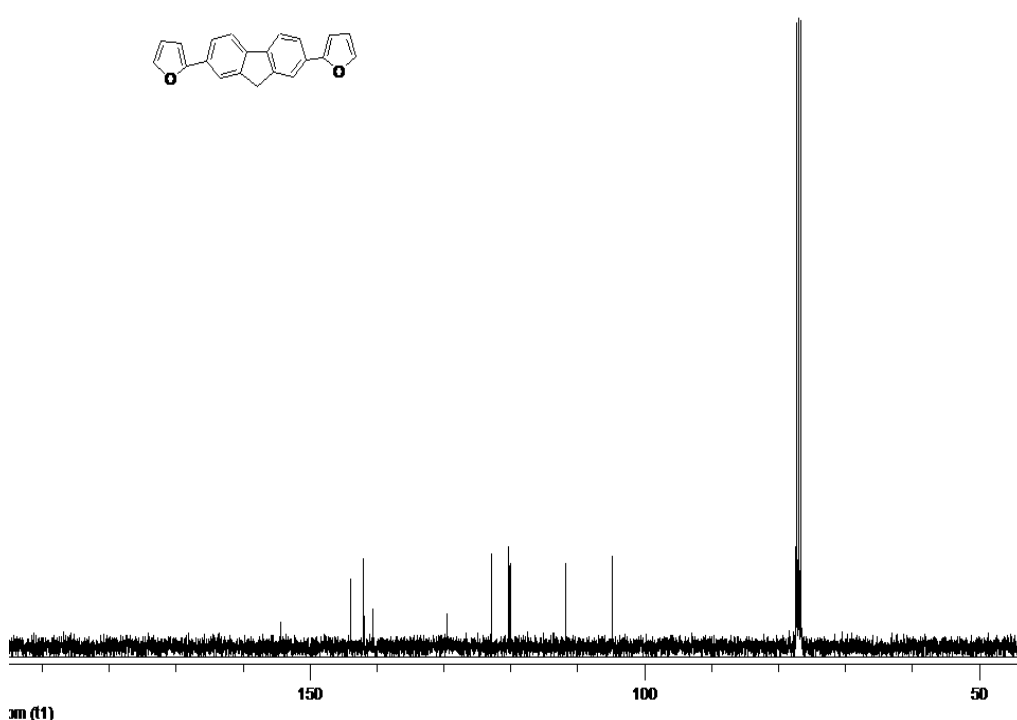
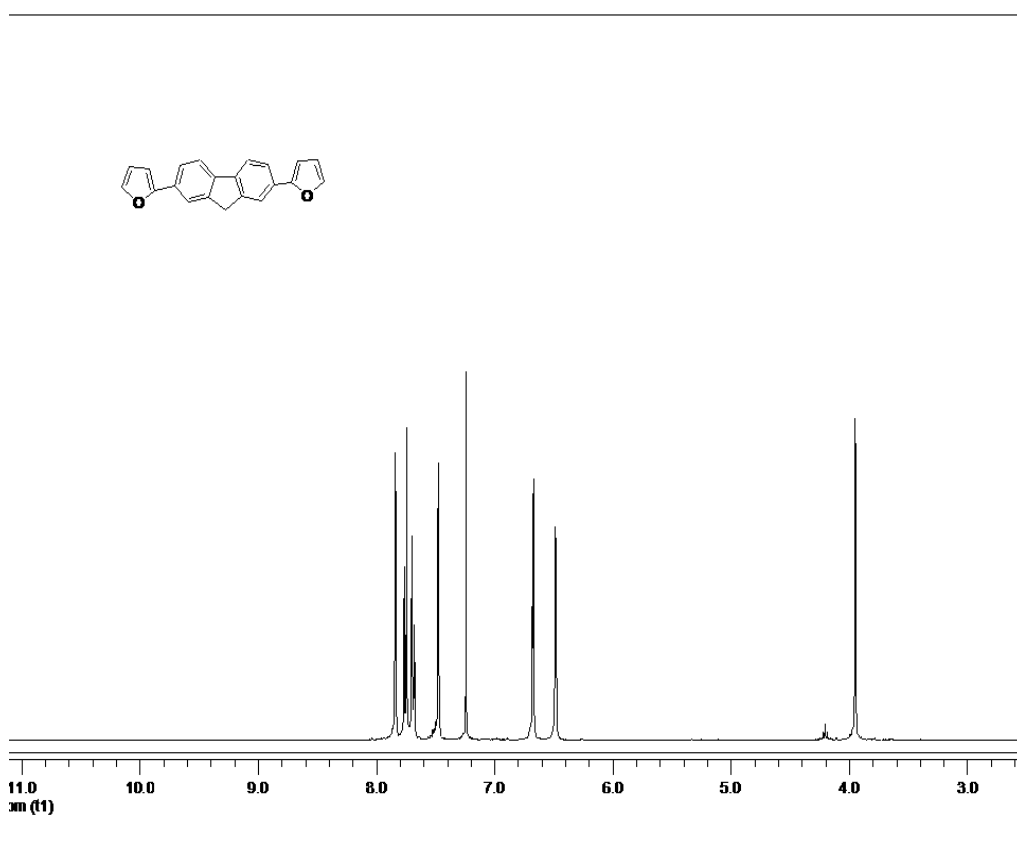


Figure A.2 ¹H NMR and ¹³C NMR of FFF.

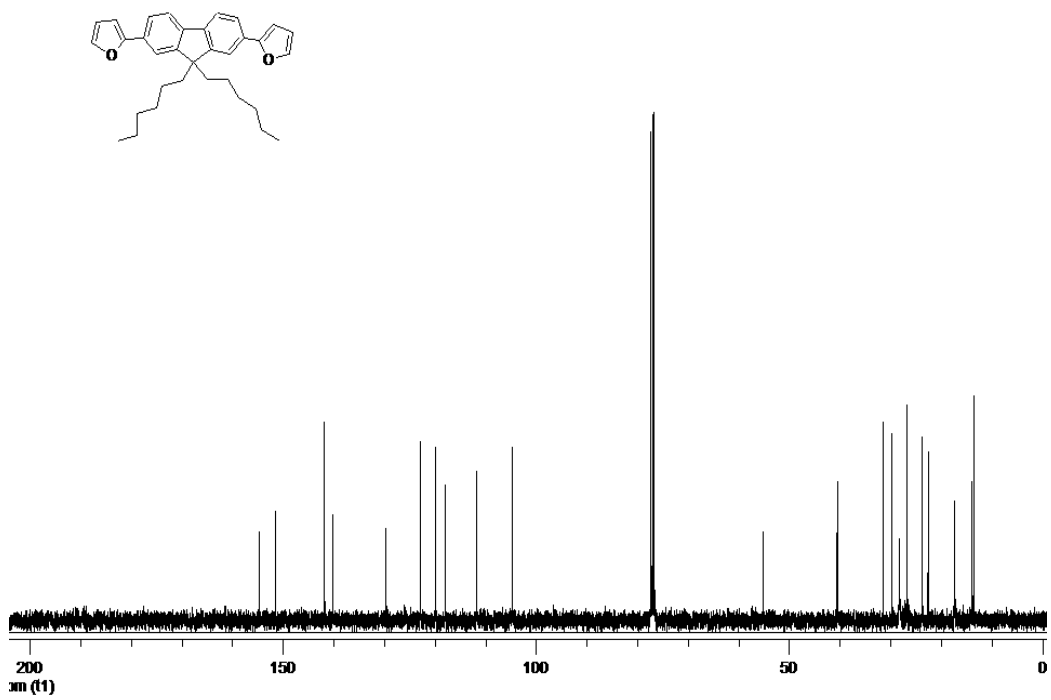
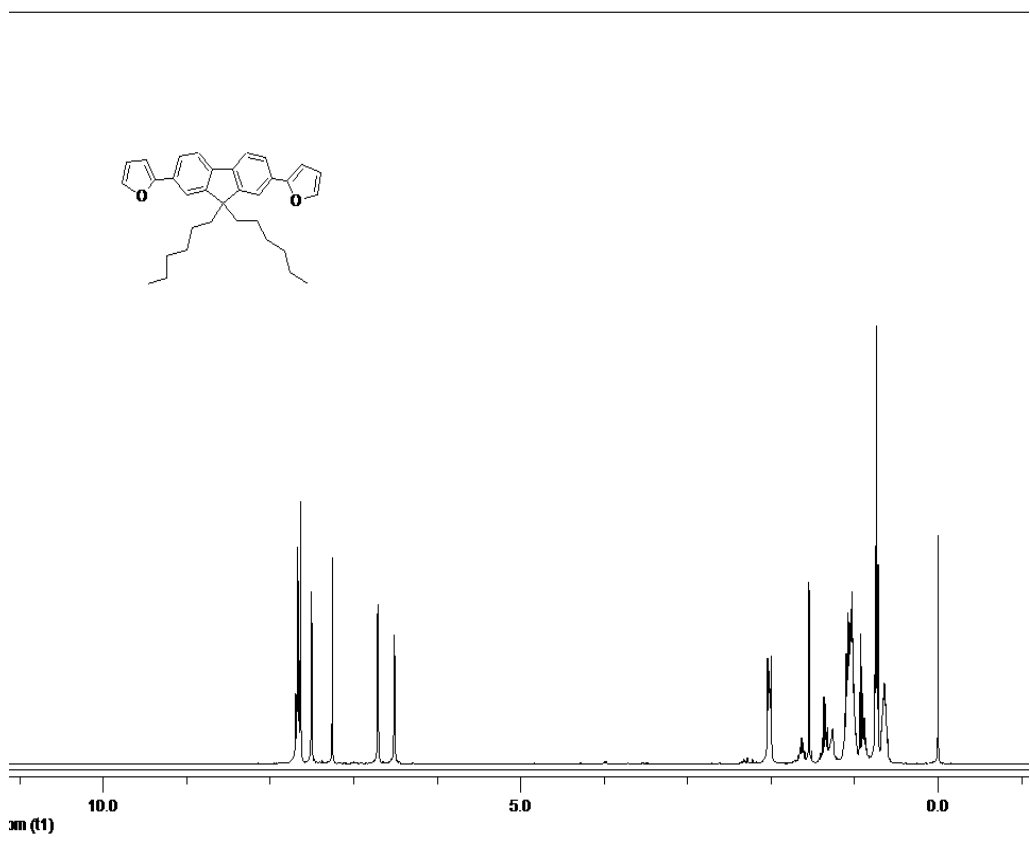
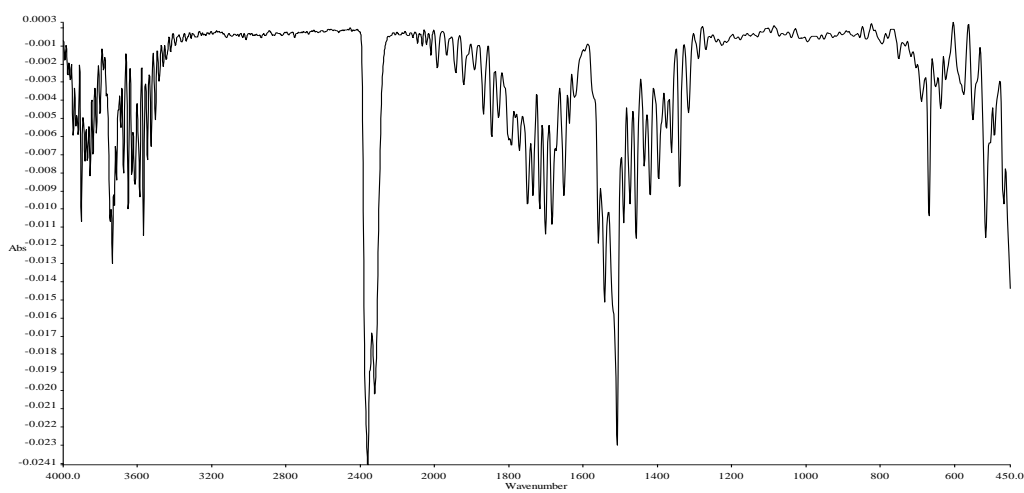


Figure A.3. ^1H NMR and ^{13}C NMR of FHF.

APPENDIX B

FTIR SPECTRA OF OUT-COMING GASES DURING TGA FOR POLYMERS; PFOF, PFFF AND PFHF

After 92 secs (45 °C)



After 5506 secs (947 °C)

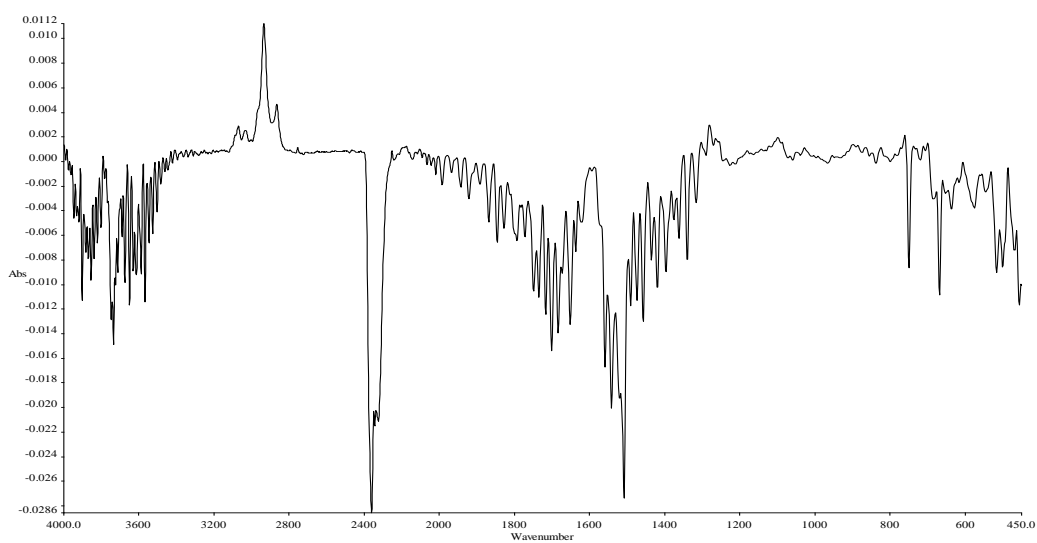
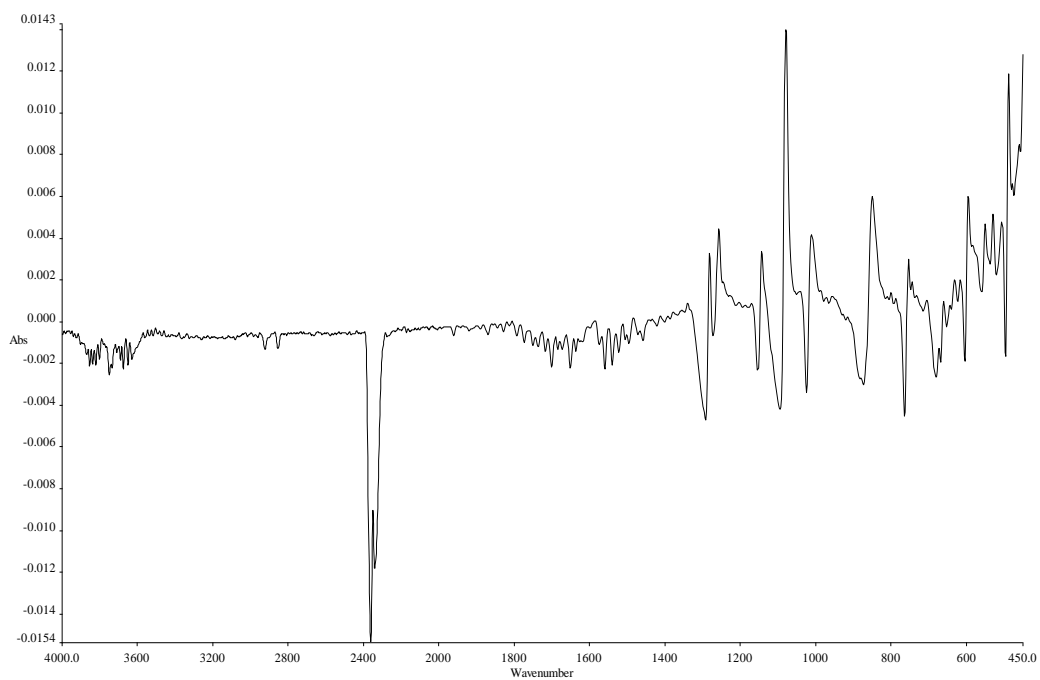


Figure B.1. FTIR Spectra of gases out-coming in TGA for PFOF.

After 43 secs (37 °C)



After 5459 secs (939 °C)

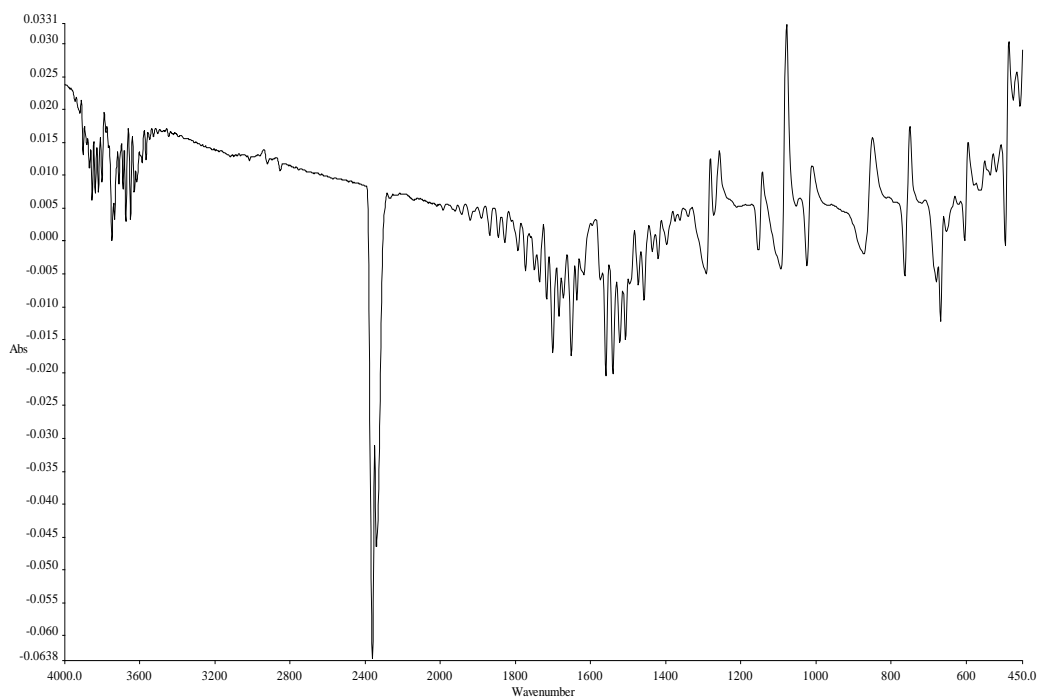
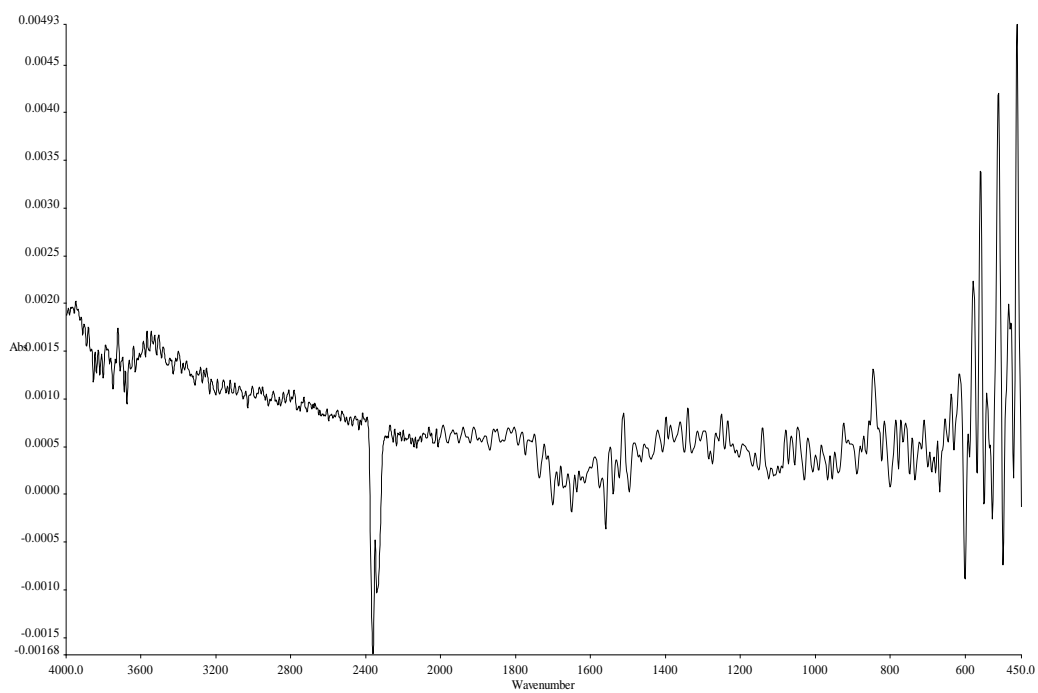


Figure B.2. FTIR Spectra of out-coming gases in TGA for PFFF.

After 90 secs (45 °C)



After 4948 secs (855 °C)

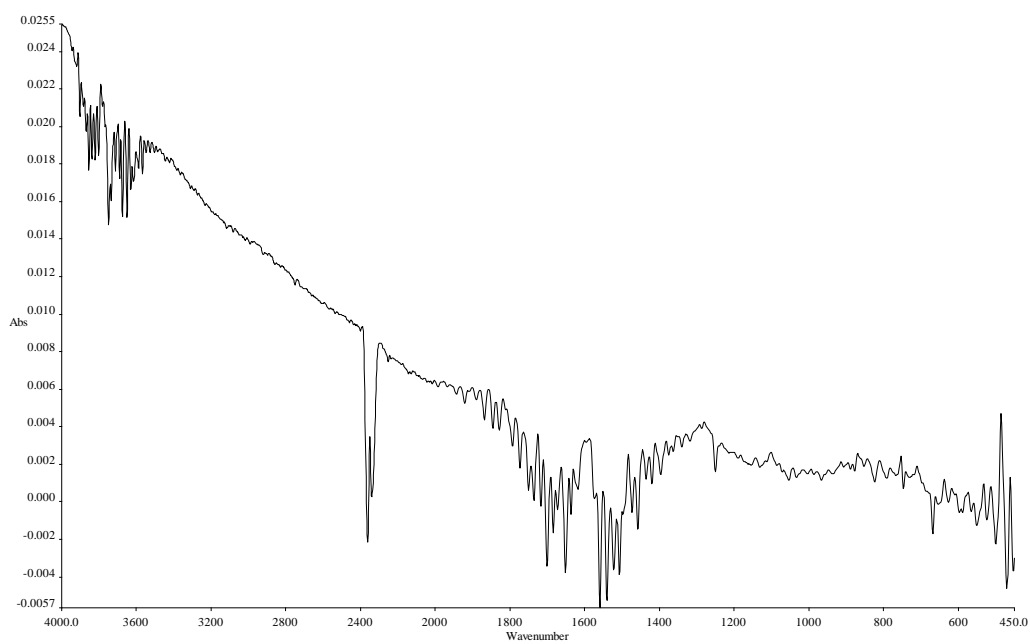


Figure B.3. FTIR Spectra of out-coming gases in TGA for PFHF.

APPENDIX C

FTIR SPECTRA OF FHF AND PFHF

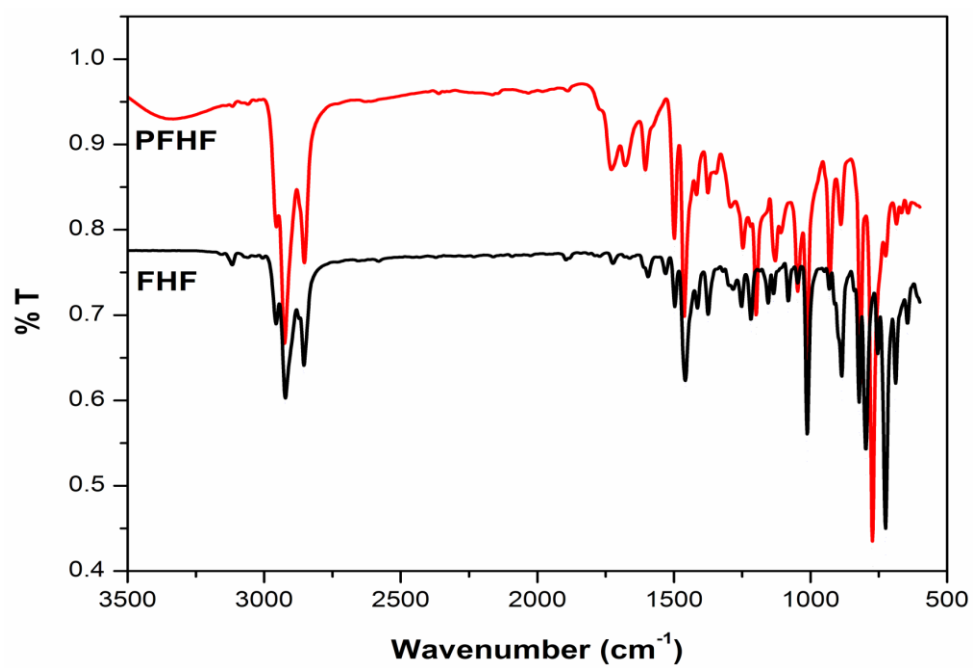


Figure C.1. FTIR Spectra of FHF and PFHF.